

A Computational Model for Predicting Visual Acuity from Wavefront Aberration Measurements

by
Azadeh Faylienejad

A thesis
presented to the University of Waterloo
in fulfillment of the
thesis requirement for the degree of
Master of Science
in
Vision Science

Waterloo, Ontario, Canada, 2009

©Azadeh Faylienejad 2009

Author's Declaration

I hereby declare that I am the sole author of this thesis. This is a true copy of the thesis, including any required final revisions, as accepted by my examiners.

I understand that my thesis may be made electronically available to the public.

Abstract

The main purpose of this thesis is to create and validate a visual acuity model with experimentally obtained aberrations of human eyes. The other motivation is to come up with a methodology to objectively predict the potential benefits of photorefractive procedures such as customized corrections and presbyopic LASIK treatments.

A computational model of visual performance was implemented in MATLAB based on a template matching technique. Normalized correlation was used as a pattern matching algorithm. This simulation describes an ideal observer limited by optics, neural filtering, and neural noise.

Experimental data in this analysis were the eye's visual acuity (VA) and 15 modes of Zernike aberration coefficients obtained from 3 to 6 year old children (N=20; mean age= 4.2; best corrected VA= 0 (in log MAR units)) using the Welch Allyn Suresight instrument. The model inputs were Sloan Letters and the output was VA. The images of Sloan letters were created at LogMAR values from -0.6 to 0.7 in steps of 0.05. Ten different alphabet images, each in ten sizes, were examined in this model. For each simulated observer the results at six noise levels (white Gaussian noise) and three levels of threshold (probability of the correct answer for the visual acuity) were analyzed to estimate the minimum RMS error between the visual acuity of model results and experimental result.

Our statistical results show that the Pearson Correlation is 0.56 and 2-tailed p value is 0.011 which demonstrates that the model tracks the variations in acuity with aberration.

Even though this study is limited to children's eyes it can be extended to adult data and can be used to objectively predict potential benefits of customized corrections using photorefractive treatment modalities.

Acknowledgements

At very first I would like to express my sincerest appreciation to Dr. Lakshminarayanan for his encouragement and support. It has been a great honor to have him as my supervisor. I would like to thank my committee members, Dr. William R. Bobier and Dr. Marlee Spafford, for their assistance. I am extremely grateful to my very best friend Roham Farzami at the Physics department. This thesis would not have been possible without his very helpful assistance in programming the Model. I was truly fortunate to have my fiancé Ramin beside me, whose kindness means so much to me. I am exceptionally thankful to him for his continued guidance and encouragement throughout my thesis research. I would like to thank the School of Optometry and the University of Waterloo for their support, which has enabled me to pursue this degree.

Table of Contents

List of Figures	viii
Chapter 1	1
Introduction.....	1
Visual Acuity	2
Wavefront Aberrations.....	4
Zernike Polynomials	6
Aberrations Types.....	8
Defocus	8
Astigmatism	9
Spherical aberration	10
Coma.....	10
Curvature of the Field	11
Distortion	11
Interaction between Aberrations	12
Contrast Sensitivity Function.....	12
Point Spread Function.....	14
Optical Transfer Function	15
Neural Transfer Function.....	16
Frequency Scale	17
Neural Noise Levels.....	18
Metrics and Models.....	18
Acuity Model	19
Aberrations and Visual Acuity.....	21
Conclusion	23
Chapter 2.....	24
Methods.....	24
Introduction.....	24
Template Matching Model.....	25
Experimental Data	27

Sloan Letters	28
Passing through Optical Filter	29
Passing through Neural Filter	31
Frequency Scale Assessment	34
Specifying Additive Noise for Each Subject	34
Matching Rule.....	36
Normalized Correlation	36
Visual Acuity Model.....	37
Performance Evaluation.....	39
Chapter 3.....	41
Results.....	41
Visual Acuity Estimation Using a Psychometric Function.....	41
Root Mean Square Error	43
Effect of Different Parameters	45
Templates	45
Noise Level	45
Frequency Scale	47
Thresholds for Visual Acuity.....	47
Mean Optical Transfer Function.....	50
Number of Matching Trials	51
Visual Acuity RMS error vs. Different Orders of Aberration	52
Chapter 4.....	54
Discussion.....	54
a. Template Matching Algorithm.....	54
b. Contrast Sensitivity in Children Eyes.....	54
c. Alternative Single Valued Metric	55
d. Visual Acuity of Preschool Children	55
e. Effects of Noise.....	57
f. Effects of Infra Red vs. Visible Light on VA.....	57
g. Different MOTFs	58
h. Using Adaptive Procedures in Template Matching.....	58

i. Running the Simulation on a Larger Population	58
Conclusion	59
Appendices.....	60
Appendix A.....	60
MATLAB Simulation Codes	60
Main.m.....	60
make_initials.m.....	62
Make_WA.m.....	63
Zernike.m	63
Make_PSF.m.....	64
Make_OTF.m.....	65
Make_CSF.m	65
Make_MOTF.m	66
Make_MOTF_avg90.m	66
Make_NTF.m.....	67
Make_template.m.....	68
match_normxcorr2.m.....	68
Appendix B	69
PSF and OTF Images	69
Appendix C	76
Calculated data to plot psychometric function.....	76
References.....	86

List of Figures

Figure 1: LogMAR high contrast visual acuity chart	3
Figure 2 : Formation of Wavefront aberration.....	5
Figure 3: WA map obtained from 20/20 visual acuity over a 5 mm pupil diameter.	6
Figure 4: Ten Zernike modes.....	8
Figure 5: Contrast Sensitivity Function.	14
Figure 6: Modulation Transfer Function for two different pupil diameters.	16
Figure 7: Simple model of human eye recognition process.....	21
Figure 8: Letter acuity template matching flowchart.....	26
Figure 9: WA(x,y) map - VA=6/6, J=14, age=6.....	29
Figure 10: Example of PSF simulated by the model for the subject#28 with VA=6/6.	30
Figure 11: Example of OTF simulated by the model for the subject#28 with VA=6/6.	31
Figure 12: 3D presentation of SCSF simulated by the model.	33
Figure 13: 3D Presentation of MOTF used to make the NTF.	33
Figure 14: 3D Presentation of NTF calculated from dividing SCSF to MOTF.....	33
Figure 15: Each subject's RMS error as a function of the neural noise.	35
Figure 16: An individual trial	38
Figure 17: A retinal letter image (Top left); Image passed through NTF filter (Top right)	39
Figure 18: Simulation using aberrated letters as the template	42
Figure 19: RMS error for subject#4 as a function of noise level.....	46
Figure 20: Sample of frequency scale as a function of RMS error for specific subject#28.	47
Figure 21: Estimated and experimental average values of visual acuity for 20 subjects.	48
Figure 22: Correlation between Data and Model; Threshold 0.66	49
Figure 23: Correlation between Data and Model; Threshold 0.60	49
Figure 24: Correlation between Data and Model; Threshold 0.50	49
Figure 25: NTF from the first method (MOTF average of OTFs of all the subjects).....	50
Figure 26: Correlation between 5 time repeating trials vs. Single trial.	52
Figure 27: Correlation between 2nd, 3rd, 4th order and total Wrms aberration with VA RMS error.....	53

Chapter 1

Introduction

According to the American Association of Ophthalmology 80-85% of a person's learning is through the visual pathway, and therefore having optimal visual performance is crucial in the learning process [1].

High-contrast visual acuity is a common clinical measure of visual performance. Recent advances in the development of wave-front guided refractive surgery have greatly increased the importance of finding a link between optical quality and aberrations of the eye [2, 3 and 4].

Today due to the development of viable clinical wavefront aberrometers, measuring the monochromatic aberration of the human eye is routinely possible, (e.g. using Hartmann-Shack methods [5],[6]), but accurately predicting visual acuity and hence visual performance that results from a measured set of aberrations has not yet been achieved and this is an area of considerable interest [7]. One reason for developing such a detailed description of the optics of the eye from aberrations is the potential to obtain highly accurate automated prescriptions of sphero-cylinder corrections (the spectacle Rx) as well as objective measurements of visual acuity.

Developing a computational model which objectively determines the best correction of the eye based on measurements of aberration would solve this problem, and could have many clinical applications. One example of clinical application is predicting the potential benefits of customized corrections with photorefractive treatments. Such a model should also have an acceptable degree of correlation with experimental results.

An important question is whether the objective method correctly estimates the best subjective refraction of the observer's eye. This objective method should take into account the effects of

higher order aberrations of the eye when estimating refraction. This is because, even though eliminating second order aberrations minimizes the root mean square (RMS) wavefront error, this minimization does not necessarily optimize the quality of the retinal image.

Thus another motivation for this study derives from the need for an alternative single valued metric instead of RMS to quantify the effects of aberrations on acuity tasks. This metric should show us the visual consequences of low levels of wave aberrations remaining after customized refractive surgery.

Previously Watson and Ahumada [7] described a template matching model that includes optical and neural filtering, and neural noise for predicting visual acuity. They found an excellent account of acuity in the presence of various aberrations. The aberrations they examined were controlled simplified combinations of second and fourth order aberration coefficients [7].

Naturally, aberrations of the human eye include more than just these two orders of aberrations, and therefore assessing the visual acuity metric and model with aberrations of real human eyes is worth pursuing. This is the purpose of the research described in this thesis.

Visual Acuity

The spatial resolution of the visual system is usually evaluated using a simple measure of high contrast visual acuity. Visual acuity shows how well an observer can see fine details and it depends on the ability of the eye to resolve a given visual angle. Most tests vary the angle by changing either the size of the stimuli or its distance from the eye. A normal visual acuity test consists of a number of high contrast, black-on-white letters of progressively smaller size. The smallest letter that can successfully be read is referred to one's visual acuity [9], [10].

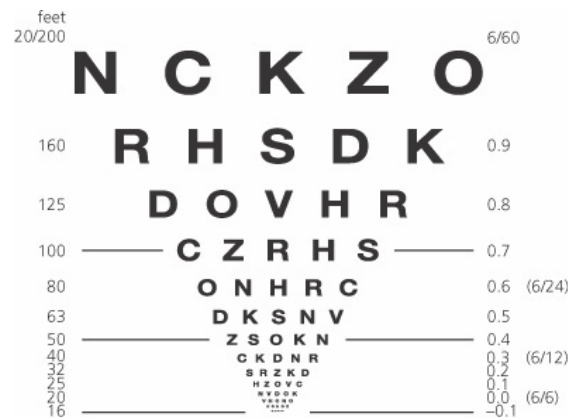
Results of visual acuity are recorded as a fraction known as the Snellen fraction. In the Snellen fraction the numerator represents the observer's distance from the stimulus and the numerator divided by the denominator represents the minimum visual angle perceived by the observer. The standard distance used for visual acuity assessments is twenty feet or 6 meters. A visual acuity of

20/20 (6/6) indicates that the observer recognizes a stimulus whose lines subtend one minute of arc at a distance of 20 feet [9].

Different types of visual acuity may be considered depending upon the specific task or detail to be resolved. The most familiar visual acuity task is recognition. The task evaluates the observer's ability to recognize and name various sized letters or symbols. The smallest recognizable letter indicates the minimum angle of detail that can be resolved [10].

Snellen charts are the most common among a variety of recognition task charts that have been developed. The charts are composed of rows of letters or symbols in progressively smaller sizes and are commonly used in eye clinics. One type of Snellen chart is shown in Figure 1. A method of measuring high contrast visual acuity to various levels of aberration is to count all letters read correctly until a set number of letters are not seen, typically five letters. Then the total number of letters read correctly is converted to a visual acuity score [11].

In the case of retarded populations or young children who do not have the necessary language skills or understand the instructions required for such tests, a reliable and accurate method for visual acuity assessment needs to be developed. Cambridge Uncrowded cards, FPL (forced preferential looking) and Teller cards are examples of experimental measurements of visual acuity in these situations.



Reference: © 2005 Elsevier Ltd. Spalton et al: Atlas of Clinical Ophthalmology 3e

Figure 1: LogMAR high contrast visual acuity chart

Wavefront Aberrations

In optics, rays and wavefronts are used to describe the propagation of light waves. Rays describe the path along which the light travels and a wavefront is a surface of points with identical phases (constant optical path length (OPL)) made by the tips of the rays. The optical path length is defined as the product of the geometric length of a ray and the refractive index of the medium. The rays of light are always perpendicular to the surface of the wavefront at every point of the surface [12].

Wavefronts radiate outward in a homogeneous medium in spherical shapes while they are concentric to the source. When the refractive medium changes the shape of wavefront will not be spherical anymore.

In a perfect optical system the light distribution of a perfect image has the same form as that of the object but there could be a difference in size or orientation due to the magnification of the imaging system [12]. There could be a shift in phase as well but this is important only for certain very off-axis situations or for highly aberrated systems.

A perfect optical imaging system gathers rays from a point source and then converges them to a point called an image point, but in the case of an imperfect optical system no point image can be formed. The reason is that in an imperfect optical system the OPL is not the same for all of the rays.

In an imperfect optical system, the light distribution in the image space is different from its distribution in the object space. The difference between these two light distributions makes a blurred image. One cause of a blurred image is aberrations. When the wavefront is aberrated it means it deviates from its perfect shape and the same phase points are not on a perfect spherical or plane surface any more. This is schematically shown in Figure 2. It could be seen in the figure that a surface of points with identical phases when passing through exit pupil (imperfect optical system) is not a spherical surface any more.

The wavefront aberration is usually measured in micrometers but sometimes in wavelengths between an actual wavefront and a reference (ideal) wavefront centered on the ideal image point [13].

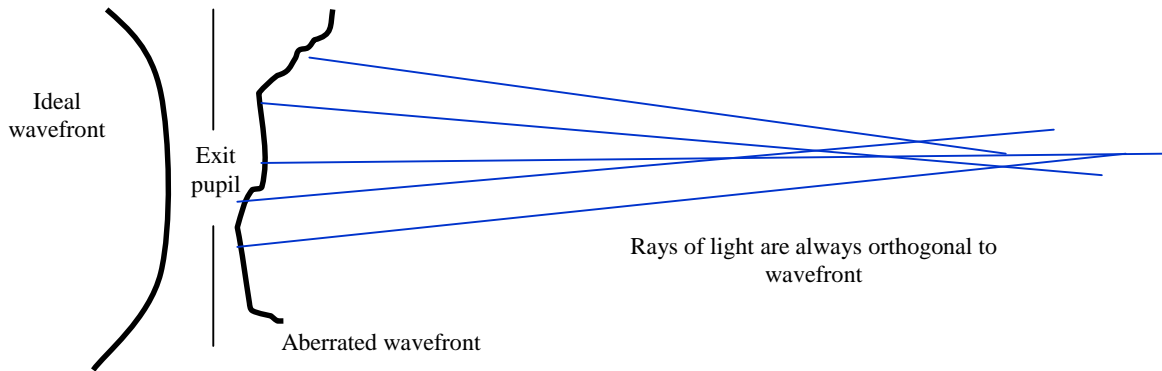


Figure 2 : Formation of Wavefront aberration

The difference between the ideal wavefront and the actual wavefront is described using a mathematically well behaved polynomial, known as Zernike polynomials. Zernike polynomials form a good orthonormal basis set of functions and are described over a unit circle. The wavefront aberrations of the eye, $W(x, y)$, can be described as shown in equation (1) [14].

$$W(\rho, \theta) = \sum_m \sum_n c_n^m Z_n^m \quad (1)$$

From these, an aberration map can be produced in order to visualize how aberrations vary across the pupil of the eye. These aberrations produce image formation errors at the retina [15].

When constructing an aberration map of the eye several formats can be used, namely, displaying them in terms of rays striking the retina, in terms of the object and retinal optical distance through different points of entry in the pupil, or in terms of the shape of the wavefront of light produced by the optical system of the human eye [16].

Figure 3 shows an example of an aberration map in terms of the shape of the wavefront produced by the optical system of a six years old subject's eye from the data set. This wavefront aberration map is computed from a set of 14 Zernike modes ($J=14$) using a model implemented in MATLAB. The color coding shows a deviation of the wavefront from the (x, y) plane perpendicular to the path of the chief ray, in μm . The color bar at the right side of the figure demonstrates numbers corresponds to each color.

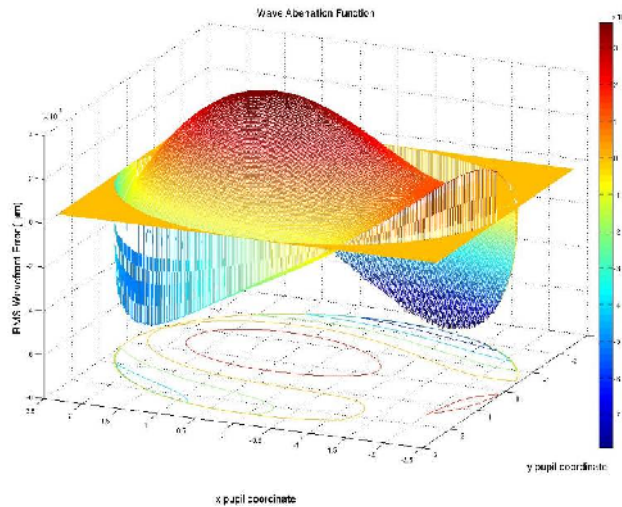


Figure 3: WA map obtained from 20/20 visual acuity over a 5 mm pupil diameter.

Zernike Polynomials

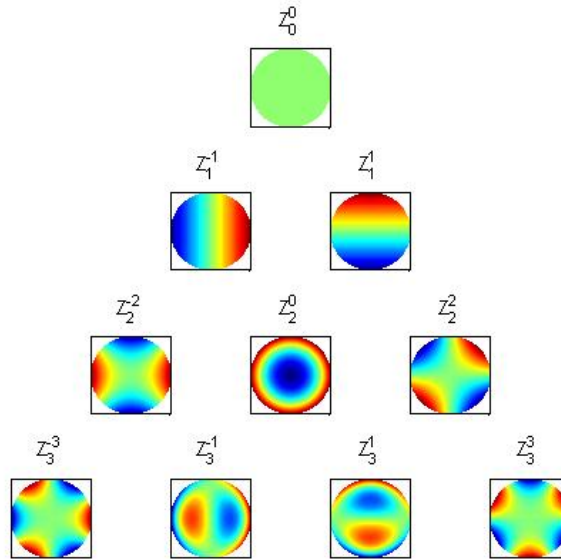
Using normalized Zernike polynomial expansions is a standard method [16] for mathematical expression of eye wavefront aberration (wavefront error). These polynomials are based on circular geometry and are ideal for describing the wavefront aberrations of the eye considering that the eye pupil has circular geometry as well. All the aberrations coefficients in Zernike's expansion, except for one, have a zero mean error for computational simplicity [16].

They also have useful mathematical properties such as completeness, orthogonality, and are normalized [16]. Their completeness means that any wavefront function $W(\rho, \theta)$ can be expressed as a linear combination of Zernike polynomials. Orthogonality implies that all Zernike polynomials are independent from each other which simplify fitting the polynomials to the wavefront. Therefore each aberration coefficient c_n^m can be obtained independently. Normality indicates that the pupil radius ranges from 0 to 1.

One advantage of describing ocular aberration with the normalized Zernike expansion is that the value of the coefficient of each mode represents the root mean square (RMS) wavefront error attributable to that mode [15].

Zernike polynomials have circular symmetry and therefore can be described in polar co-ordinates, (ρ, θ) in the pupil plane, where ρ is the radius of pupil ranging from 0 to 1 and θ is the angular component ranging from 0 to 2π .

The Zernike terms are ordered based on the power of the radial component of the Zernike polynomial. For example Z_1^1 shows a first order term with the frequency component equal to one or in Z_3^{-3} order is 3 and frequency component is -3. The first two orders represent tilt and defocus. Larger orders show higher-order aberrations and some of which are named [14]. Figure 4 shows the example of some Zernike modes.



Reference: <http://www.mathworks.com/company/newsletters/digest/2008/jan/zernike.html>

Figure 4: Ten Zernike modes.

Aberrations Types

Aberrations are divided into two general types. They are either monochromatic or chromatic [13]. In the case of monochromatic aberrations, the light is composed of a single wavelength, while chromatic aberrations occur only in polychromatic light and are due to the dispersion of the optical medium. The studies of this thesis are performed for monochromatic light therefore the chromatic aberrations will not be discussed in this area.

Monochromatic aberration shows several kinds of defects in the optical system including defocus, spherical aberration, astigmatism, coma, and curvature of the field [17], [18]. These are the third-order monochromatic aberrations that are called Seidel aberrations.

Defocus

Defocus simply means out of focus or the axial deviation from the best focus location. Optically it refers to a condition in which the image is not formed on the focal plane (surface of best focus) but at a point longitudinally displaced from it.

Generally defocus reduces the sharpness and contrast of the image, hence fine details of images are blurred or even indistinguishable. Nearly all eye optical systems include some form of defocus. In some systems defocus is balanced with another aberration hence the combined aberration is minimized. If the eye only had defocus, then the shape of wavefronts in the image space would remain spherical but would not be centered at the image plane [18], [19].

In the Zernike polynomial expansion, the defocus wavefront aberration is indicated by the second order aberration and is shown by this coefficient: C_n^m where, n= order of coefficient =2, m= frequency of coefficient = 0

Astigmatism

Astigmatism can occur for rays of light coming from on-axis point objects when the optical system is not symmetric about the optical axis. The human eye often exhibits this form of aberration due to imperfections in the shape of the cornea or the lens.

Astigmatism can also arise from an off-axis point object caused by the tilting of a wavefront relative to the optical surface [19]. When an optical system has astigmatism distortion the rays that propagate in two perpendicular planes end up at two different foci.

In the Zernike polynomial expansion of wavefront aberration astigmatism is among the second and fourth order aberrations and is shown by these coefficients:

$$C_n^m = \{ C_2^{-2}, C_2^2, C_4^{-2}, C_4^2 \}$$

Spherical aberration

This kind of aberration happens when the marginal rays of the light source come to a shorter focus than rays of light from the central portion. This shifting of focal length for different rays of light is caused by deviations in the surface of the optical system of the eye (lens or cornea) from an exact sphere. This aberration can be inferred as an excess or lack of peripheral refractive power that creates a symmetrical blur circle of light around a point image. [19]

When an optical system has more power peripherally its corresponding spherical aberration (SA) is called under-corrected or positive. On the contrary, if an optical system has less power peripherally then its SA is referred to as overcorrected or negative [17].

In the Zernike polynomial expansion of wavefront aberration, spherical aberration is indicated by the fourth order aberration and is shown by this coefficient: $C_n^m = C_4^0$
n= order of coefficient =4, m= frequency of coefficient = 0.

Coma

Coma is another type of distortion, in the phase of light entering the eye, due to non optimal surface shape and misalignments in the optical elements of the eye.

Coma occurs when a bundle of light rays entering an optical system is not parallel to the optic axis. It is a variation of image magnification with radial distance of incident rays from the optical axis. In general, coma wavefront aberration results from tilting the incident wavefront with respect to the optical surface, or axial displacement from optical surface. The image of a point source looks like the coma tail of a comet, hence the name. Coma forms when the refractive surfaces have asymmetrical shapes or when the optical elements are misaligned with respect to the optical axis [17].

The coma effect is frequently combined with other aberrations, such as astigmatism and chromatic aberration. In the Zernike polynomial expansion of wavefront aberration, coma is indicated by the third order aberration and is shown by these coefficients:

$$C_n^m = \{ C_3^{-1}, C_3^{+1} \}$$

Curvature of the Field

This type of monochromatic aberration can simply be defined as an optical system imperfection in which the objects at the edge of the field of view can not be brought into sharp focus at the same time as the objects in the center, and vice versa[18].

Curvature of field is an aberration that makes an extended object focus on a curved surface instead of a flat image plane. Almost all optical systems suffer from field curvature, which is a function of the refractive index of the optical elements and their curvature of surface. The image surface is almost spherical near the optical axis and is called the Petzval surface.[16], [17].

If a flat image surface focuses the on-axis point of the object surface then the image of off-axis points have circular blur since they are defocused at this plane. The level of defocus increases with the distance of the off-axis point. Field curvature can be corrected with the right combination of surface shapes and their refractive indices [19]. One solution could be making the object or image recording surface curve to compensate for field curvature.

Field curvature has same order and frequency as defocus in the Zernike terms expansion.

It is indicated by C_2^0 .

Distortion

Varying image magnification with the distance from the optical axis causes distortion. The more off-axis is an object point, the larger is the change in magnification.

Distortion deforms the image as a whole; hence it is the most easily recognized aberration. It has two types: pincushion and barrel distortion. When the magnification increases with off-axis position, the distortion is named as positive or pincushion distortion. When the magnification decreases with distance from the optical axis, it is called negative or barrel distortion.

In the Zernike polynomial expansion of wavefront aberration, distortion is indicated by the first order of aberration and is shown by these coefficients: $C_n^m = \{C_1^{-1}, C_1^1\}$.

Interaction between Aberrations

Mathematical independence of the Zernike modes does not mean that their impact on visual performance is also independent [20]. Interaction between Zernike modes causes increase or decrease in the optical quality of the eye. In some situations, a slight aberration in the eye can provide some relative visual benefits [21], therefore two combinations of wavefronts with the same value of RMS error, could result in a different image quality, and consequently different visual acuity. This fact shows that RMS is not a good metric for predicting visual acuity from wavefront aberrations [14].

One aberration could be applied to interact with another such that the resultant improves the modulation transfer function (MTF), and consequently improves image quality. This is known as aberration balancing. The Zernike modes which have the same signed coefficients with two radial orders apart (e.g., radial orders 1 and 3) and have equal angular frequency (e.g., angular frequencies -1 , or 1) can be combined such that the effect on acuity is less degrading than each by itself. These combinations, when in correct proportions, reduce the wavefront error over the center of the pupil [20], [21]. An application of interaction between aberrations is when using aberration combination to make the spherical aberration to nearly zero using two or more lenses in collimated, monochromatic light.

Contrast Sensitivity Function

The Contrast Sensitivity Function (CSF) is a measure of the ability of the visual system to see detail at various contrast levels. It is a plot of sensitivity (defined as the inverse threshold) as a function of spatial frequency. The contrast sensitivity function tells us how sensitive we are to the various spatial frequencies in the visual stimuli. If the spatial frequency of visual stimuli is very high we will not be able to recognize the stimuli pattern any more since it will be beyond the resolution limit [22, 23]. For example, if an image consists of very thin vertical black and white stripes, we can not distinguish the pattern any more.

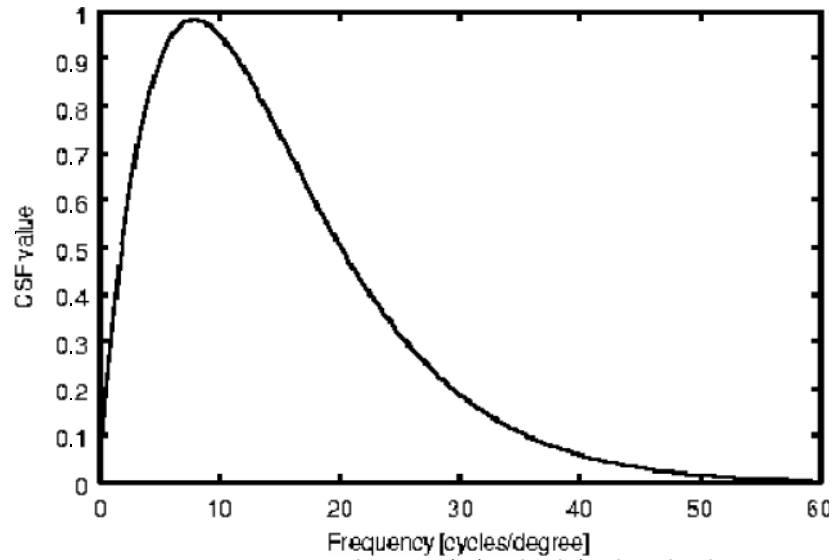
Contrast is created by the difference in luminance between the light and dark bars. It is usually quantified by equation (2) and is also known as Michelson contrast and is usually expressed as a percentage. If l_{\max} = maximum luminance (the lighter surface) and l_{\min} = minimum luminance on (the darker surface), then contrast is defined as:

$$\text{Contrast} = \frac{l_{\max} - l_{\min}}{l_{\min} + l_{\min}} \quad (2)$$

When the darker surface is completely black it reflects no light, the ratio (contrast) is 1.

Among the people with normal sight this function has a maximum (normalized) value of approximately 1, at $f = 8.0$ cycles/degree, and is meaningless for spatial frequencies above 60 cycles/degree. The Contrast Sensitivity Function has neural and optical components. The MTF is the optical contribution to the contrast sensitivity function (CSF) and neural transfer function is its neural part. [24, 25]

The contrast sensitivity function (Figure 5), shows how sensitive the visual system is to the various spatial frequencies contained in the visual stimuli.



Reference: www.cg.tuwien.ac.at/~matkovic/node20.html

Figure 5: Contrast Sensitivity Function.

The reason that the human eye can not distinguish patterns with high frequencies is believed due to the limited number and dimensions of photoreceptors in the eye. It is also limited by the sampling characteristics of the photoreceptors and the multiplexing between the photoreceptors and the underlying neural substrates such as ganglion cells.

The Contrast sensitivity function is impacted by the presence of the aberration of the eyes. Yamane et.al [26] demonstrated that induced changes in the contrast sensitivity function significantly correlated with increases in ocular higher order aberrations.

Point Spread Function

The Point Spread Function (PSF) is one of several metrics used to describe the optical quality of the eye or any optical system. Point spread function represents the response of an imaging system to a point object. As a result of being imperfect optical systems, the stimuli undergo a certain amount of degradation, when visual stimuli are passed through the cornea and lens and the media [23].

The PSF shows this image degradation, represented as a plot of relative intensity of a point of light, as a function of distance from the center of the retina. In other words, PSF is the irradiance distribution of a single point source, which shows the degree of blurring of the point object, when projected onto an image plane.

There are number of reasons for the image of a point source not being just a point any more. First, aberrations in the optical system will spread the image over a finite area. Second, diffraction effects will also spread the image, even in a system that has no aberrations [22]. Scattering in the media will also play a role.

The Fourier transform of the PSF is called the Optical Transfer Function. In other words PSF is the spatial domain version of the optical transfer function (which is in the frequency domain) [22].

Optical Transfer Function

Optical transfer function presents the relation between the image produced by an optical system and the amplitude and phase of an object at various spatial frequencies.

It can show how well the contrast has been transferred from object to image. The OTF is a complex function; its real term gives the ratio of amplitudes, and the imaginary term gives the phase relationship between the object and the image. [25, 26]

The modulus or absolute value of the optical transfer function is called the modulation transfer function (3).

$$OTF(\eta, \gamma) = MTF(\eta, \gamma) * PSF(\eta, \gamma)$$

Where

$$MTF(\eta, \gamma) = |OTF(\eta, \gamma)| \quad (3)$$

$$PSF(\eta, \gamma) = \exp(-i2\pi\lambda(\eta, \gamma))$$

The MTF is the ratio of image contrast over the object contrast as a function of spatial frequency. It can be seen in Figure 6 that the eye can not distinguish features smaller than one minute of arc (60 cycles per degree). The value of MTF drops down when pupil radius increases.

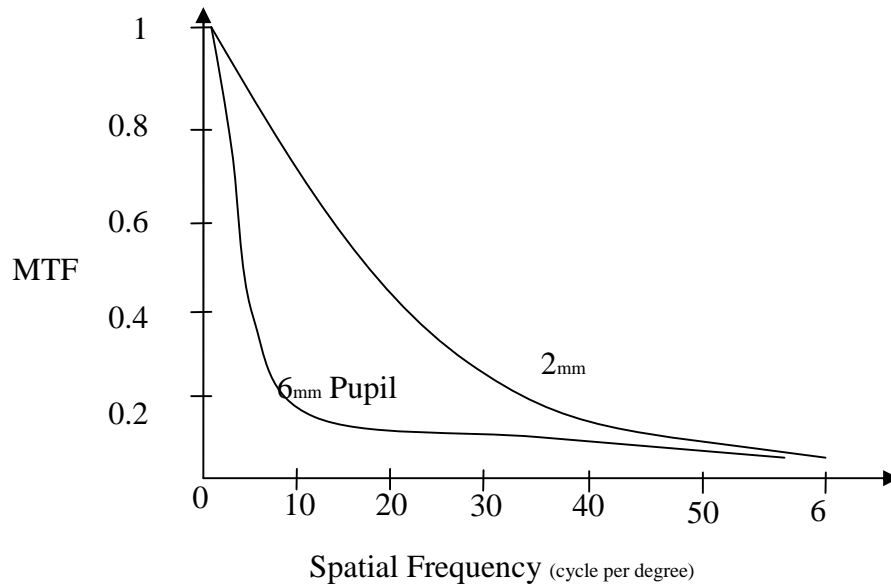


Figure 6: Modulation Transfer Function for two different pupil diameters.

Neural Transfer Function

When rays of light from an object are imaged the retina, they are captured by photoreceptor cells, which transform the light into electrical impulses, to carry out to the brain by the optic nerve, for final visual processing. The mathematical function that has been developed to show this process is a Neural Transfer Function (NTF). The neural transfer function is also sometimes called neural contrast sensitivity function.

NTF shows how well the retinal image is interpreted by the neural portion of the visual system. The overall contrast sensitivity function of the eye is the product of optical and neural transfer functions. This can be seen by the fact that the low frequency fall off in sensitivity seen in the CSF can be attributed to receptive field organization of neural cells in the retina and beyond. Therefore

the neural transfer function can be derived if one has values of contrast sensitivity function and optical transfer function [7].

Usually a standard form for CSF is defined, and then the optical component of the function is removed. The remaining function is the neural transfer function, which shows the ability of a visual system to transform visual information to the brain [27] and is given by equation (4).

$$NTF = \frac{CSF}{OTF} \quad (4)$$

Frequency Scale

Using a standard contrast sensitivity function and a mean value for the optical transfer function to measure neural transfer function provides a fixed value for NTF [28, 29]. Usually different observers have different neural transfer functions (NTF); therefore a parameter should be included in the computation to show possible variations in the neural transfer functions for different observers. Thus the value of the neural transfer function would be more accurate for each observer [7].

A frequency scale, α , is used for this purpose. This scale, α has the effect of shifting Standard Contrast Sensitivity Function (SCSF) horizontally in the amplitude vs. spatial frequency coordinates. The result is the shifting of the neural transfer function to the higher values which mean better ability of the neural transfer function in transferring information from higher spatial frequencies to the brain. Consequently higher values of the frequency scale demonstrate higher values of acuity.

This method of randomly varying the value of neural transfer function has the advantage of providing a single parameter that can control the most important aspect of NTF, i.e. its sensitivity at higher spatial frequency [7].

Neural Noise Levels

For the same stimulus, different subjects can have different thresholds (or sensitivities). This is due not only to the criterion used by the subjects but also due to the presence of different amounts of neural noise. Hence, the model should incorporate a parameter that takes into account noise in the neural system. Therefore, in addition to the frequency scale the other parameter that governs the performance of the acuity model is the amount of neural noise σ_n , [7]. Trial and error are the best way of finding the proper value of σ_n for each subject. Thus for each individual a sequence of values of σ_n should be tested to find the best fitting value. It is clear that each observer has a different σ_n . Generally this estimation of σ_n should be in agreement with the empirical result in the observer's sensitivity. In this simulation the noise is taken as always zero-mean Gaussian noise. Therefore the nature of the noise does not change; only the amount of it is variable [7]. The reason of existence of this free parameter in the model is to make discrimination between subjects' neural sensitivities.

Metrics and Models

A distinction should be introduced between metrics and models. Metrics consist of computations or equations that describe quantitative relationships. Metrics can quantify the results in measurable terms. On the other hand, models include dynamic statements that attempt to clarify why the relationship exists [7].

A model is a symbolic representation of the basic structure of an object or event in the real world. Modeling is used as a tool to explore the obscure workings of complex systems. Commonly, the greater the number of simplifying statements made regarding the basic structure of the real world, the simpler the model [31].

The goal of a scientist is to create simple models that have a great deal of descriptive power. The relation between aberrations and visual acuity of the human eye is an example of such a model.

Metrics may have more practical advantages due to their simplicity, while models present a scientific purpose [31].

To find a link between aberrations and visual acuity, at least four types of metrics and models can be used depending on the expected accuracy we are looking for in the result.

The simplest ones are the metrics and models that incorporate only optics. For example the RMS error of the wavefront takes into account only the optics of the eye. The second types are metrics and models that include some explanation of post-optical (neural) processing. Approximately all of the acuity models that have been developed previously are of these first two types [31].

One step forward is having the metrics or models that include the defined acuity targets, such as Sloan letters, in the computation.

The last and most complete are metrics and models that also simulate the particular task undertaken in the acuity measurement, like identification of each Sloan letter. The model and the metric that will be using in this dissertation both fall into this last group.

The model and metric are designed to predict letter acuity from wavefront aberrations. The model is a Monte Carlo simulation [30] of a decision process and its component is an ideal observer limited by optics, neural filtering, and neural noise. The metric is a deterministic calculation including optics, letters, and a theoretical neural transfer function.

Acuity Model

Practically and theoretically it has been always a matter of interest how humans can distinguish between the letters of the alphabet. The principles that have been discovered in the study of letter recognition could be generalized to perception of more complicated types of letter discrimination

and feature analysis. The numerous proposed theories on letter discrimination could be divided into two general categories: feature-based and image-based theories [33].

In the feature-based theories, the hypothesis is that letters are identified through their component features like horizontal lines or concave curves, etc. But the feature-based models neither indicate the method by which the image of the letter is transformed into features nor do they describe the nature of the features, or the processes involved in mapping features onto abstract letter characters.

Therefore feature-based models are not regularly applied for example in font design. Image-based models measure the luminance image of the letters. Both models have a common defect. They are not well generated by basic principles of pattern recognition; consequently they do not work accurately [33].

Here a “minimal” image-based model is used. In other words its measurement is based on luminance image of the letters. A minimal model is one which is as simple as possible and only contains the processes that are essential. For that reason implementing (and running a simulation) a program based on a minimal model, takes less time than for complex models. The overall structure of the recognition process of the model is illustrated in Figure 7.

The main and unavoidable components are Sloan letter image, optical and neural filters of the eye, and normalized correlation (matching component). The optical and neural filters represent the limited resolution of the visual system. As demonstrated in the Figure 7, first an image passes through filters and then the matching process is applied on a result of noised filtered image. If the model does the correct match the letter of output is same as the input letter image.

The model is implemented in the digital image domain. Inputs and outputs of the model at every stage are discrete finite digital images. Details about this model are explained in chapter 2 of this thesis.

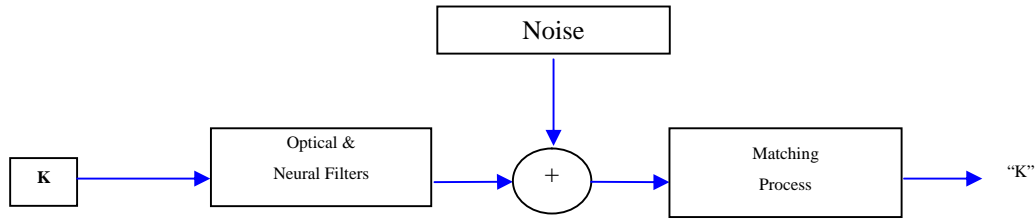


Figure 7: Simple model of human eye recognition process.

Aberrations and Visual Acuity

In this section, the literature on the relationship between acuity and wavefront aberrations is briefly reviewed. Applegate et.al [8] have measured letter acuity for three observers in the presence of 34 different combinations of two Zernike modes whose total RMS error was fixed at $0.25 \mu\text{m}$, over a 6.0 mm pupil. Although the RMS wave-front error was constant, the performance varied by up to 0.2 Log MAR values (logarithm of minimum angle of resolution). Therefore The RMS wave-front error and the equivalent defocus ($M_e = \frac{4\pi\sqrt{3}RMS}{pupilArea}$) are not good predictors of visual performance.

In conclusion they mention that visual acuity varies significantly depending on which Zernike modes are included in the analysis and their relative contributions. Modes of two radial orders apart in the Zernike expansion can be combined to improve visual acuity. They also pointed out that the RMS is not a good predictor of visual acuity for low levels of aberration while previous studies showed that for high levels of aberrations RMS is a good predictor of visual performance.

Guirao and Williams [35] have examined seven metrics to calculate the impact of high order aberrations of the eye on subjective refraction. Their metrics were divided to two types, pupil plane metrics and image plane metrics. The pupil plane metrics calculated the wave-front over the pupil and image plane metrics consisted of calculations in the retinal image plane. They collected

aberration data and subjective refraction in different settings for 146 observers. They concluded that their image plane metrics presented good prediction of refraction while the quality of the pupil plane metrics declined as higher order aberrations increased, and that higher order aberration influenced the amount of spherical and cylindrical correction required.

Cheng, et al. [36] have studied the impact of higher-order monochromatic aberrations on lower-order subjective spherocylindrical refractions. In their experiments visual acuity (VA) was determined while monochromatic computationally-aberrated, Sloan letters were viewed by an observer through a 2.5mm pupil. Then they compared the results to the prediction of 31 metrics. Their results showed that presence of fourth order aberrations changes the effect of defocus; in other words the amount of defocus required for the best acuity depends on the amount of higher order aberration. Several of the metrics that they examined correlated well with measured letter acuity.

Thibos, et al [32] have assessed the ability of the same metrics in addition to two other metrics to predict best refraction. They used the aberration map of 200 subjectively corrected eyes. They simulated subjective refraction by computationally varying spherical and cylindrical corrections for each metric and each map, in order to maximize the predicted acuity. Then the resulting simulated correction was compared with the actual correction. They found that among all metrics only five were reasonably accurate.

Marsack, et al have compared the experimental results from Applegate, et al [18] to compute the values of 31 metrics that Thibos, et al [29] assessed. These investigators changed the distribution of 0.25 μm RMS wavefront error across the pupil and measured the correlation of 31 metrics of optical quality to high contrast visual acuity. The best metric was found to be the VSOTF (Visual Strehl ratio Optical Transfer Function) which accounted for 81% of the variance. The VSOTF is the contrast-sensitivity-weighted OTF divided by contrast-sensitivity-weighted OTF for diffraction limited optics.

Conclusion

The simplified Visual Acuity Model (Figure 7) proposed here is an attempt to find an alternative value for RMS wavefront error to predict visual acuity from 14 modes of wavefront aberrations of the eye. The elaborated Visual Acuity Model is explained in more details in the next chapter.

The reason for the challenge to seek such a model is to find an automated objective measurement of visual acuity and of automated prescription of sphero-cylindrical corrections that provides the best visual acuity.

Chapter 2

Methods

Introduction

As noted earlier, visual acuity is the most broadly used metric to describe the quality of an individual's overall visual performance [10]. To subjectively evaluate people's visual acuity a standard eye chart is required [11]. The Sloan letter chart is a logMAR chart and is used in low vision studies frequently.

Sloan Visual Acuity (VA) is measured by asking the subject to recognize the targets. The minimum size of the targets for which the number of correct answers is above a specified threshold determines the subject's visual acuity. This visual acuity is usually expressed as a LogMAR (Logarithm of the Minimum Angle of Resolution) value.

Sloan VA has a high sensitivity to optical imperfections such as aberrations. It can detect defocus values equal to or less than $\frac{1}{4}$ Diopter (D) [38]. Unfortunately this measurement does not give any information about the amount or type of the higher order aberrations involved.

Based on the recognition task of Sloan visual acuity, Watson & Ahumada [7] have proposed an acuity model to objectively predict visual acuity from the total aberrations of the eye. They examined controlled simplified combinations of a second and a fourth order aberration and found an excellent account of acuity in the presence of those aberrations.

In this thesis a model was implemented using MATLAB based on Watson and Ahumada's idea to develop a computational acuity model. As aberrations of the human eye include more than just two orders, this implemented visual acuity model assessed the real aberrations of the eye up to 14 terms of aberration.

Template Matching Model

I have applied an instance of a “Template Matching” model for the algorithm of the visual acuity model I have implemented. This model presents an excellent fitting match with experimental data while having very few assumptions, parameters and calculations. It is a simple model while meeting all the conceptual requirements of a visual acuity model as previously described in Chapter 1.

The basic conceptual requirements of an acuity model are specific target images, optical and neural filters of the images, an additive neural noise, and a set of template letters to perform the matching process. The Sloan letters are an example of a specific target image set. The additive neural noise simulates a biological task which always includes some natural noise. It is known the brain maintains certain level of noise to optimize visual acuity performance.

Usually after several exposures to the alphabet letter patterns, over a number of years, a person’s brain constructs templates for those patterns. The template matching model assumes that, several same shapes, but perhaps different size and patterns of each particular letter are stored in the brain [31]. Recognition consists of finding the best match between a target letter and one of these templates in the brain.

Figure 8 shows the overview of this acuity model. Its components include a digital Sloan letter image as the input, two optical and neural filters, that this letter image passes through, an additive Gaussian white noise, and a set of template images. These templates are compared with the noisy neural image. One set of templates is used for each candidate letter to select the closest match. Finally the output is the visual acuity of a subject in LogMAR value.

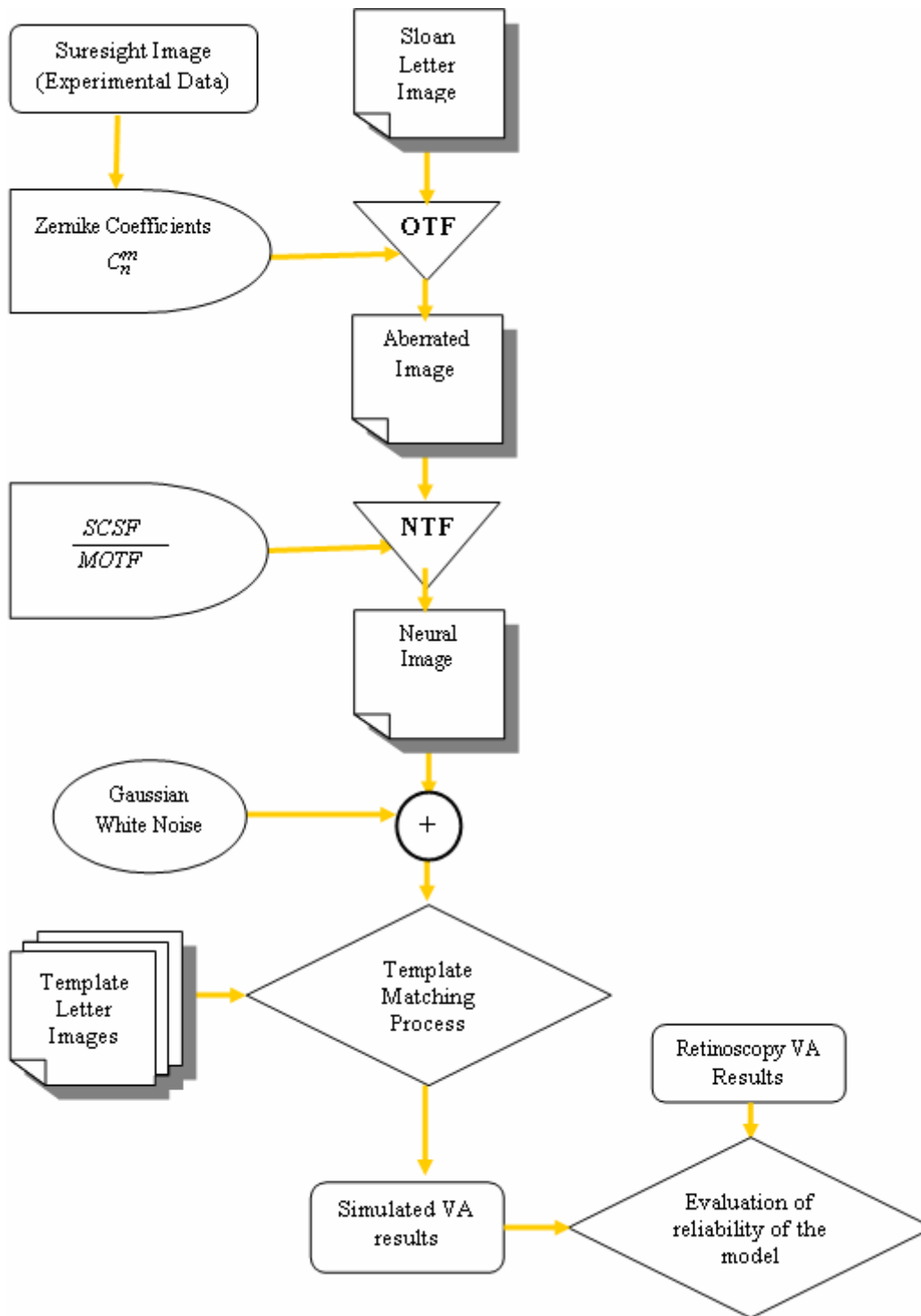


Figure 8: Letter acuity template matching flowchart

For a template matching model three types of templates could be considered: the original letters, the neural images of the aberrated letters, and the neural images of the diffraction-limited letters.

The original letter template type corresponds to a subject who retains templates with minimal optical degradation. These templates may be learned at a larger size and then mentally scaled down to the suitable size. The neural images of the aberrated letters template type corresponds to subjects who retain templates from prior experiences of the letters passed through the optics of their eyes. The diffraction-limited letters template type is appropriate when an observer's brain stores the patterns of the letters under diffraction limited conditions.

Experimental Data

Three to six year old pre-school children were chosen as the subjects of this study. (N=20; mean age= 4.2 years; best corrected VA= 0 (in log MAR units)). These subjects were part of a larger school screening study conducted by Dr. W.R. Bobier of the School of Optometry at the University of Waterloo. Two sets of data were used in this computational model. The image of each subject's eye was used to calculate aberration coefficient of the eye and the subjective visual acuity of each subject was used to evaluate the performance of this model.

The first set of data, are the images of each subject's eye. An aberrometer, Welch Allyn Suresight®, was used to capture these images. This instrument is based on the Hartmann-Shack aberrometer principles [5, 6]. Welch Allyn Suresight® image data is used by MATLAB language software to calculate up to 64 modes of aberration coefficients. This software finds the aberration (Zernike) coefficients by independently fitting each Zernike polynomial term to the eye wavefront. These aberration coefficients were obtained by courtesy of my college Damber Thapa (Vision Science graduate student, University of Waterloo, Canada). The Optical Transfer Function (OTF) of the acuity model was then calculated from these coefficients.

The other set of data, the subjective visual acuity, was obtained from Cambridge Uncrowded Cards. This test does not require the subjects to name the letters. They should only match the test letters with the letters on matching board. The single letter testing was conducted in this

experimental study not the crowded acuity test. The subject was at a distance of 3 meters from the cards.

In order to evaluate the performance of the model, these empirical results for visual acuity were compared with the visual acuity achieved from the computational model. The RMS error between the two visual acuities is then calculated.

From approximately 2000 three to six year old, Oxford country pre-school children (data collected from 2001 to 2006), I have randomly selected subjects from 2006 data (subject's eye images were taken by the Welch Allyn Suresight® autorefractor, software dev 2.2), among all age groups to create a set of 20 subjects (10 boys and 10 girls) pupil images of the right eye and visual acuities.

Data shows that most of the children in this study are hyperopic, because the optical structure of young children's eyes is not completely developed yet. The mean pupil size of the subjects was 5.6 mm, ranging from 2.2 to 6.9 mm. The mean spherical equivalent (= spherical power + 0.5 * cylindrical power) was 1.19 D, ranging from -1.90 to +4.77D.

Sloan Letters

Sloan letters are the test images of the model. They are ten letters of the English alphabet (Z, R, K, D, C, V, N, O, S, and H). The experimental visual acuity is measured using Cambridge Uncrowded Cards. The letters of Cambridge Uncrowded cards are U, X, O, H, V, T and A. The images of Sloan letters used in the acuity model were created using Mathematica software. These images were 256 x 256 pixels, with a resolution of 313.91 pixels per degree; consequently the images subtended 0.815 degrees.

Each of the ten alphabet images used in this model created in 27 sizes, in units of LogMAR value. The letter size varies from LogMAR -0.6 to 0.7 with a step size of 0.05 resulting in a total of 27 different sizes. The letters are black on a white background. In the simulation, the image pixel values are scaled to real numbers in the range 0 to 1. Zero is black and one is absolute white.

Passing through Optical Filter

A visual system can be divided into optical and neural parts. Optical Transfer Function (OTF) and Neural Transfer Function (NTF) are the corresponding parts of the visual acuity model. To get the aberrated retinal image, each letter image of the Sloan chart, is first filtered by OTF, the optical filter of the eye. Then to generate the neural image of the Sloan letters, it is filtered by NTF, the neural filter of the eye.

To calculate the OTF of a subject's eye, the first step is finding the Zernike coefficients (aberrations coefficients) from the image of the eye. These coefficients are used to calculate the two dimensional wave-front aberration functions, $WA(x, y)$. This function is used to compute the generalized pupil function, $GP(x, y)$. Figure 9 Shows an example of calculated $WA(x, y)$ map for a six year old subject with a 5mm pupil and a standard visual acuity (6/6).

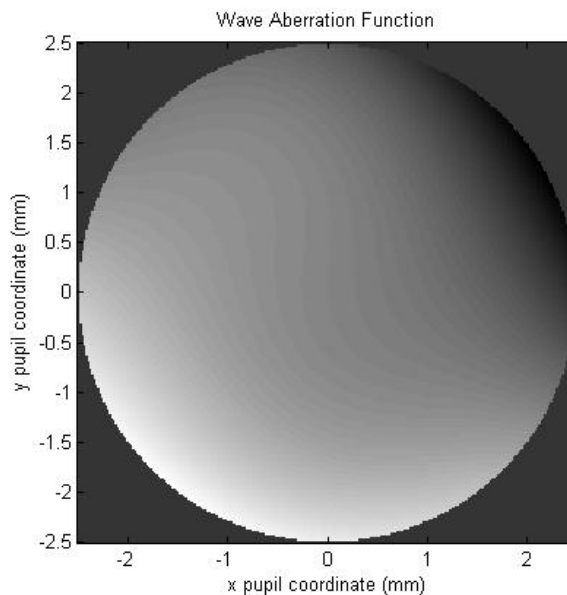


Figure 9: $WA(x,y)$ map - VA=6/6, J=14, age=6

The eye's optical performance is characterized by the generalized pupil function, GP(x, y) (equation 5) which is a complex function that describes the wavefront at the exit pupil plane.

$$GP(x, y) = P(x, y) \exp \left[\frac{i2\pi}{\lambda} W(x, y) \right] \quad (5)$$

The pupil function P(x, y) is the transmittance (portion of photons transmitted) as a function of position within the plane of the pupil. In equation (5) the transmittance is defined as 1 where the pupil lets light through and 0 elsewhere.

GP(x,y) is used to calculate the Point Spread Function (PSF), the response of the optical part of the eye to a point source. The PSF is squared modulus of the Fourier transform of the generalized pupil image. Appendix A gives the MATLAB code for calculating PSF from GP where P is the pupil function and apw is pupil area in unit of wavelength.

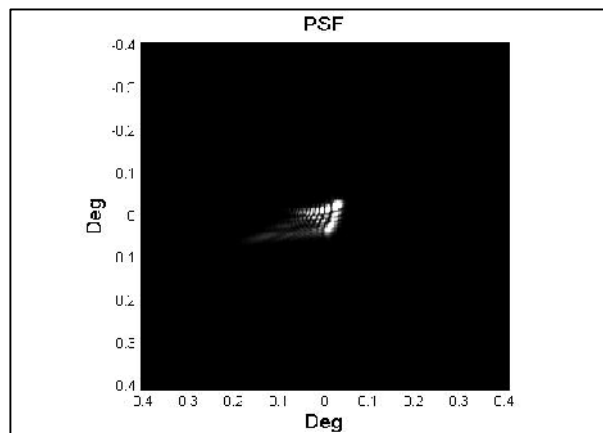


Figure 10: Example of PSF simulated by the model for the subject#28 with VA=6/6.

The letter image is convolved with PSF to obtain the aberrated retinal letter image. The spatial domain convolution is equivalent to a simple multiplication in the frequency domain. Discrete Fourier Transform (DFT) is used to change the domain from spatial to frequency. OTF is the Discrete Fourier Transform of the Point Spread Function. The aberrated retinal letter image is

obtained by multiplication of the OTF and DFT of the letter image, followed by an inverse DFT. The corresponding MATLAB code is given in appendix A.

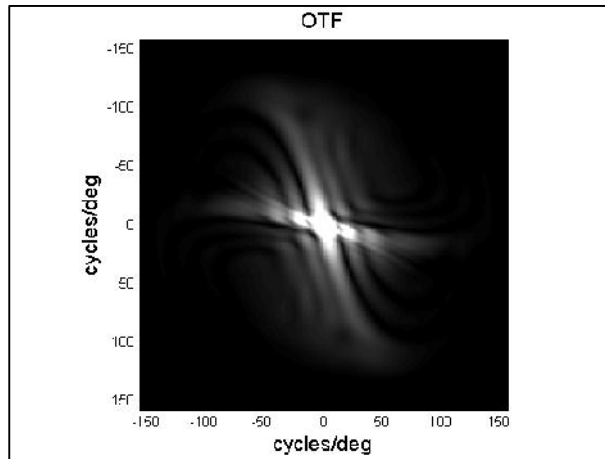


Figure 11: Example of OTF simulated by the model for the subject#28 with VA=6/6.

The PSF and OTF of all subjects are displayed in Appendix B

Passing through Neural Filter

As mentioned in Chapter One the neural filter of an image is called Neural Transfer Function (NTF). NTF indicates how well a retinal image is interpreted by the neural portion of a visual system. It is calculated by removing the optical component (OTF) from the Contrast Sensitivity Function (CSF). CSF contains both optical and neural components and is defined in the frequency domain.

By sampling the one dimensional CSF shown in equation (6) a two dimensional CSF filter is created as a discrete digital Finite Impulse Response (FIR) filter.

Among a number of different versions of the CSF a standard functional form for the radially symmetric CSF is used in this thesis as shown (equation 6).

$$SCSF(f; f_0, f_1, a, p) = \operatorname{sech} \left[\left(\frac{f}{f_0} \right)^p \right] - a \operatorname{sech} \left[\frac{f}{f_1} \right] \quad (6)$$

The CSF is a band pass function; consequently the structure of Standard Contrast Sensitivity Function (SCSF) is composed of a high-frequency lobe minus a low-frequency lobe.

The parameter f_0 scales frequency in the high-frequency lobe, the parameter f_1 scales frequency in the low-frequency lobe, and the parameter a determines the weight of the low-frequency lobe.

SCSF is divided by the Mean Optical Transfer Function (MOTF) to remove the optical component. MOTF is constructed by calculating the average of OTF matrices for all the subjects.

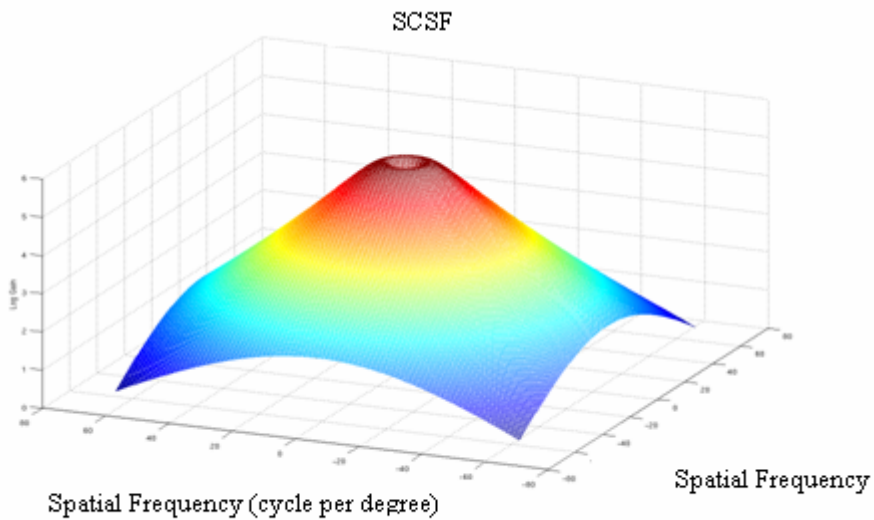


Figure 12: 3D presentation of SCSF simulated by the model.

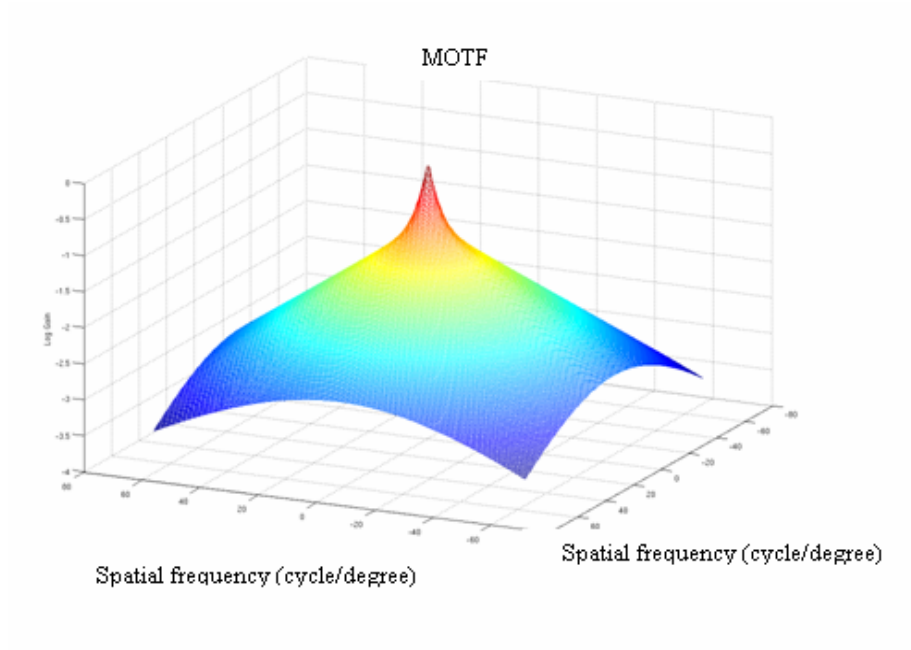


Figure 13: 3D Presentation of MOTF used to make the NTF.

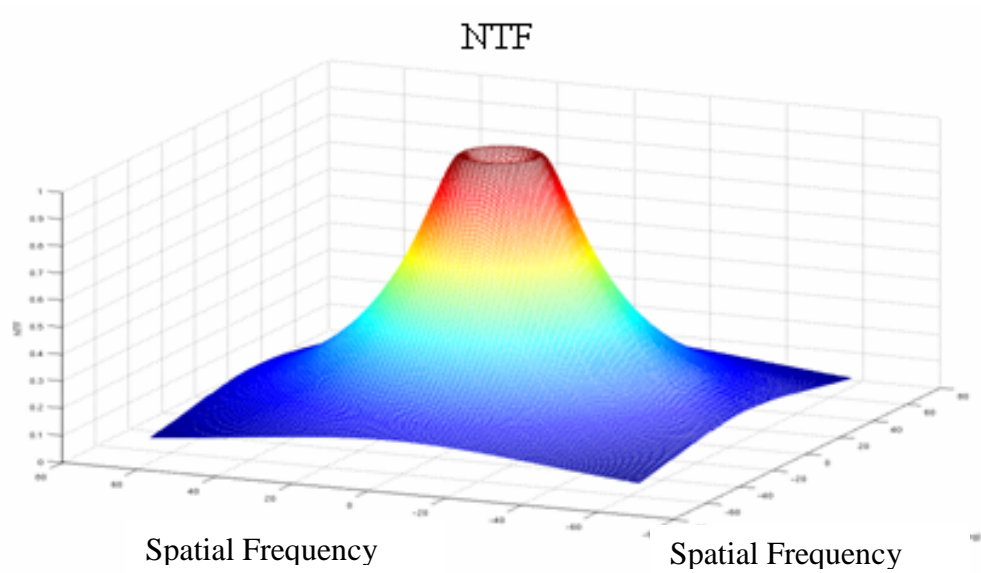


Figure 14: 3D Presentation of NTF calculated from dividing SCSF to MOTF.

Using this method results in the same NTF for every subject. We know it may not be accurate for all observers because people have different NTFs. Therefore for solving this problem a parameter “frequency scale” is introduced here.

Frequency Scale Assessment

To consider potential variations in the neural transfer functions of different observers the frequency scale multiplies the two parameters f_0 and f_1 of Standard Contrast Sensitivity Function. As previously mentioned in the introduction chapter, the frequency scale () has the effect of shifting SCSF horizontally. Consequently the neural transfer function shifts to higher values, and transfers information from higher spatial frequencies to the brain. A larger frequency scale corresponds to a higher value of visual acuity meaning the individual can see more details.

Frequency scale is a parameter that changes the value of NTF to be specific to each subject rather than being based on the average population. To find the optimal for each observer several random values for frequency scale are examined and the result of visual acuity from calculations is compared with the experimental result. Finding the optimal to get the best fit to the experimental data is somewhat arbitrary and time-consuming.

Specifying Additive Noise for Each Subject

Most biological organs have some amount of internal noise. The same applies to the neural part of the visual system. This additive noise is usually useful for vision [48]. For example in very dim light an imperceptible image can be seen due to this additive noise. The noise can exceed the threshold sensitivity and the image is perceived Therefore performance of the acuity model is

governed by the amount of neural noise. One can hypothesize that in the brain some process is implemented to generate just the right noise level where the visual sensitivity of the individual is at its maximum. In this model a zero-mean Gaussian white noise is added to the neural image to simulate this additive noise.

A computational model that is as similar as possible to the real natural biological procedure is needed to find the optimum noise level for each subject.

A simple technique for finding the right noise level for each subject, is to find the smallest Root Mean Square (RMS) error between the experimental data and computational model when examining several values of noise, σ_n . The noise that results in this minimum amount is the suitable noise for that person. Finding the best fit for each subject is possible at the last step of the modeling procedure after applying the matching rule and obtaining the Visual Acuity (VA) from the model. Figure 15 shows an example of finding the best noise level for four subjects based on the minimum RMS error.

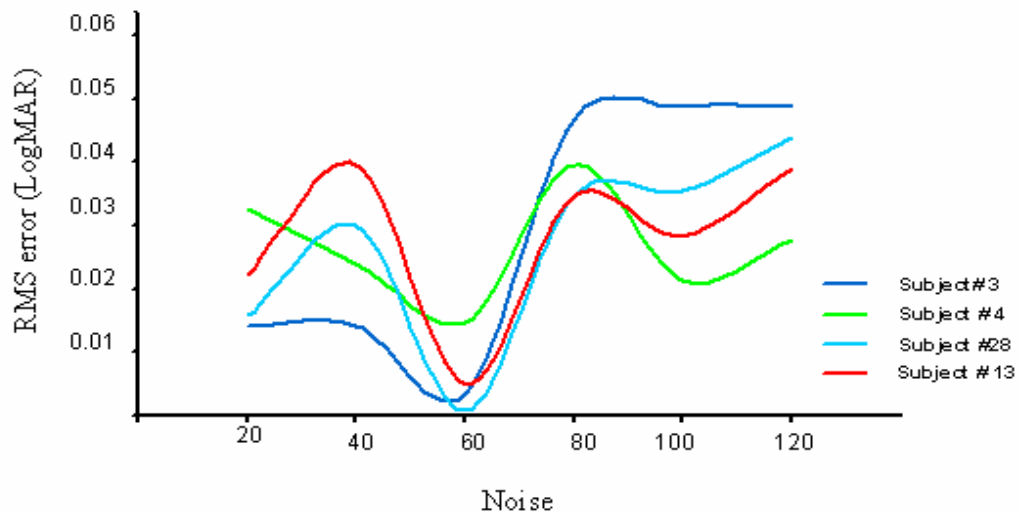


Figure 15: Each subject's RMS error as a function of the neural noise.

Matching Rule

Normalized Correlation

There are several pattern matching algorithms that could be used. An experimental study of five template matching algorithms, when various image distortions are present, shows that normalized correlation presents the best performance [41]. In the normalized correlation matching rule, letter images filtered by aberrated optics and neural filter are used as templates.

The discriminant for normalized correlation is shown in equation (7). Templates are normalized but they are not perturbed by any noise. When normalization is applied the patterns will be matched on the basis of shape rather than mean value.

The test letter image $s_k(x)$ and the candidate images $t_j(x)$ differ only by a shift along the x-axis. Cross-correlation is used to find out the amount $s_k(x)+n(x)$ must be shifted along the x-axis to make it identical to $t_j(x)$. The equation slides $s_k(x)$ along the x-axis, calculating the integral of the test and the candidate image product for each possible amount of sliding. When the functions match, the value of $(\bar{t}_j(x) \otimes (s_k(x)+n(x)))$ is maximized.

$$g_j = \max (\bar{t}_j(x) \otimes (s_k(x)+n(x))) \quad (7)$$

Here, \bar{t}_j is the normalized template for the letter indexed by j.

In the Normalized correlation rule the observer is limited by optics of the eye and internal noise. The output of correlation of the test letter $s_k(x)$ and the candidate images $t_j(x)$ is itself an image, and the value at each pixel of the result image reflects the correspondence of the two other images. Taking the maximum selects the greatest correspondence.

Visual Acuity Model

The model computes visual acuity from the measured wavefront aberrations for each subject. The visual acuity is simulated in the digital image domain and is implemented in MATLAB language. Inputs and outputs of the model are discrete finite digital images. (Appendix A).

Two main factors limit the visual perception of individuals. One is the ability of the optics of the eye to form the image on the retina (optical filtering) and the other is the capability of the retina to transfer the details of that image to the brain (neural filtering).

Other parameters affect the visual acuity therefore this model is based on the letter acuity task that contains, optical and neural filtering, neural noise and a template matching rule.

In all the simulations the pupil diameter was set to a standard size of 5 mm. This is the result of using a 5 mm pupil in calculation of the Zernike coefficients from the experimental data.

Figure 16 shows the overall flowchart for an individual trial.

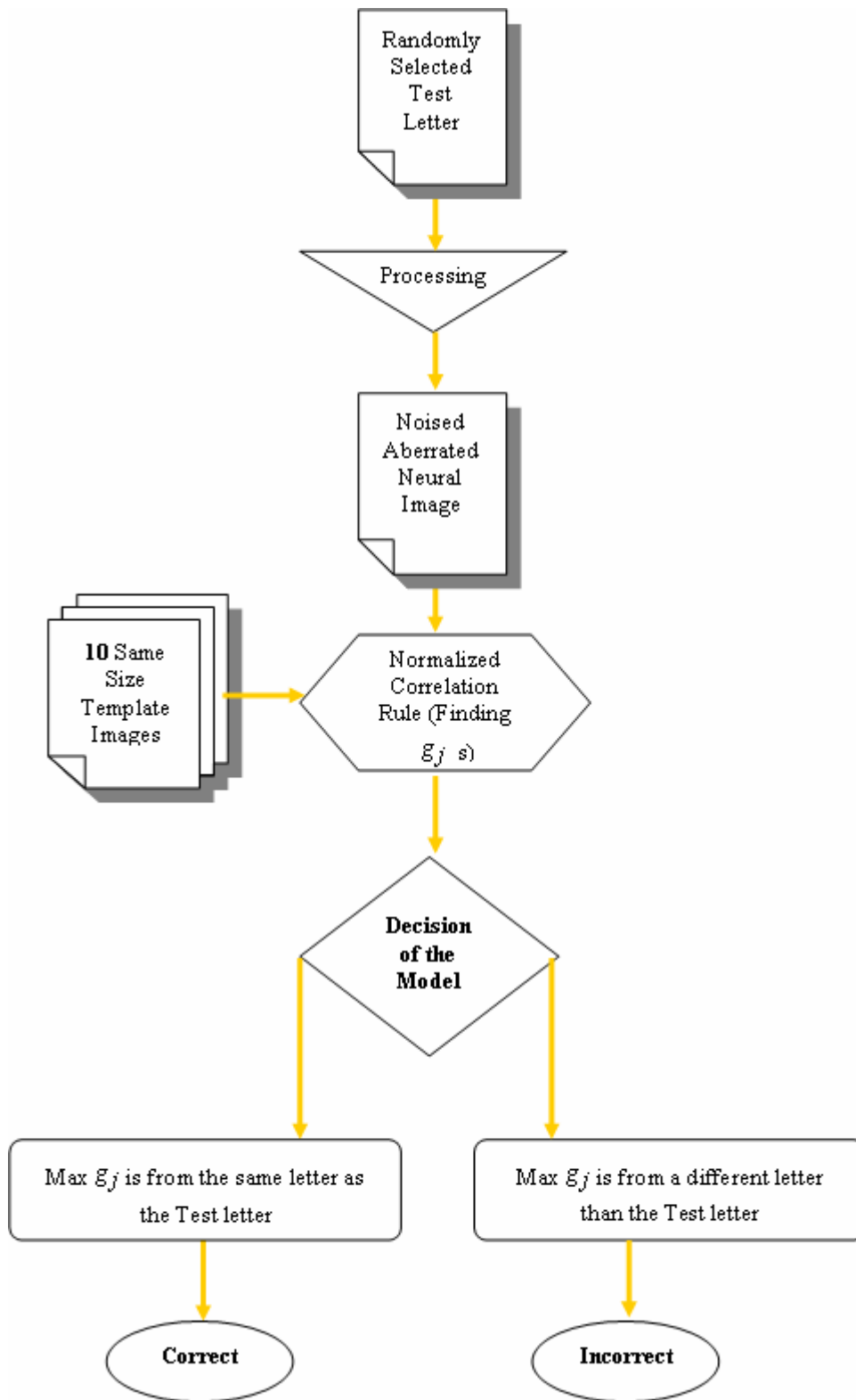


Figure 16: An individual trial

Figure 17 shows a retinal image at different steps of the model.

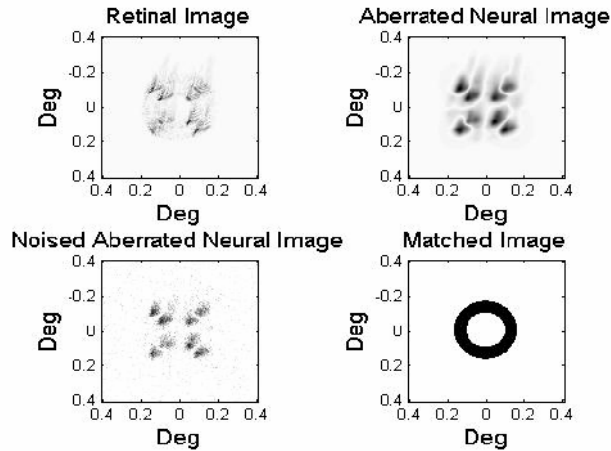


Figure 17: A retinal letter image (Top left); Image passed through NTF filter (Top right) ; Neural image with added noise (Bottom left); result of the matching process (Bottom right)

Performance Evaluation

The last step is to find out the degree that the performance of the acuity task of the model is matched with the visual acuity obtained from experimental data.

Finding the RMS error between model and data is a good measure of performance. Note that σ_n should be optimized separately for each subject, because individuals possible presentation of different average acuities. Therefore, for each observer, different values of σ_n are tested separately and the RMS error as a function of σ_n is plotted.

Every point of Figure 15 is obtained based on 100 trials at each observer's eye aberration conditions while trying to find suitable noise values. The frequency scale has a constant value of $= 1$.

Among the several σ_n s for each observer the one that presents the minimum amount of RMS error is taken as the optimized neural noise level.

More explanation of the process of finding the best RMS error for each subject is in the Results chapter of this thesis.

Chapter 3

Results

Visual Acuity Estimation Using a Psychometric Function

A psychometric function demonstrates the relationship between a physical stimulus and the responses of an individual about a certain parameter of that stimulus. Usually the psychometric function has an S-shape and is also called an ogive shape and represents a cumulative probability distribution. The y-axis represents the probability of success in a certain number of experiments at that stimulus level and the x-axis shows the value of the physical stimuli. Finding the proper range of the stimulus value is important in getting correct results from the psychometric function [44].

The stimulus should not be easily perceptible or completely indistinguishable for the subject. If the stimulus is indistinguishable, it is probable that the subject responds randomly; therefore the results of the function would not be reliable. On the other hand, if the person is always able to respond correctly then the threshold of perception of the stimulus can not be obtained since the strength of the stimulus is always above threshold. The sensory threshold is the point where a transition between correct and incorrect responses occurs.

A common application of a psychometric function is estimating subjective visual acuity using an eye chart stimulus. The subject of study observes letters of different sizes, such as in LogMAR value, on the acuity chart. These letters are the physical stimuli. As long as the subject responds correctly in distinguishing the letters, smaller sizes are tested. The line on the chart where the subject can not recognize some of the letters usually shows the sensory threshold and corresponds to the visual acuity.

In this model a similar method was simulated to estimate each subject's visual acuity. After finding the portion of correct responses for each size of the letter the data were fit by a Logistic

model of Sigmoidal Function. Using the fit plot, acuity was calculated as the value of LogMAR at which the probability of a correct response was $P = 0.66$.

An example of one simulation is shown in Figure 18. This procedure of acuity estimation was applied to each of the 20 subjects with 15 terms of aberration coefficients and 6 levels of noise. Aberrated letters were used as the template for this simulation.

Figure 18 shows the estimated acuity for an observer at noise level = 60%. The black points show the proportion correct at different letter sizes. The blue lines indicate the VA estimation as the LogMAR for which the probability correct is 0.66.

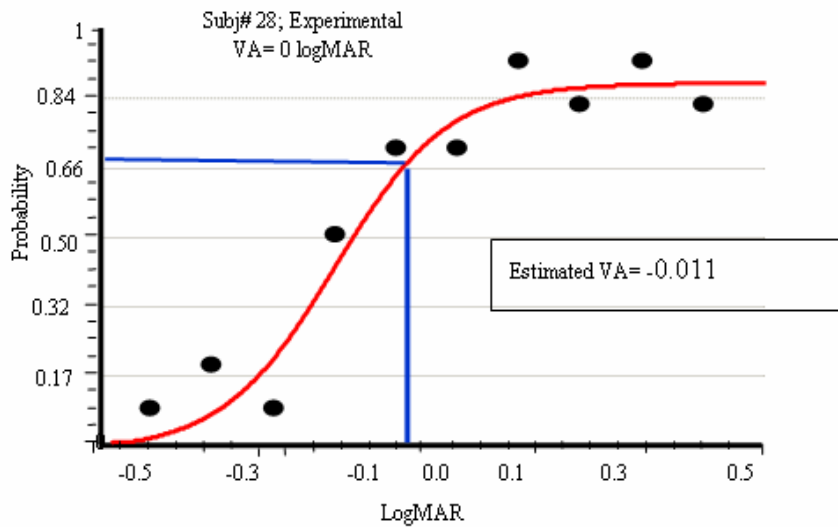


Figure 18: Simulation using aberrated letters as the template

Table 1 shows an example of the results at different sizes to plot the psychometric function for a subject.

Subj#4; VA=0							
Noise =		20	40	60	80	100	120
Letter sizes	LogMAR	Probability of Correct Response					
5	-0.4	0.3	0.3	0.3	0.2	0.3	0.4
7	-0.3	0.2	0.2	0.2	0.2	0.2	0.2
9	-0.2	0.3	0.2	0.2	0.3	0.2	0.3
11	-0.1	0.8	0.8	0.8	0.8	0.8	0.7
13	0	0.7	0.7	0.7	0.7	0.7	0.7
15	0.1	0.7	0.7	0.7	0.7	0.7	0.7
17	0.2	0.9	0.9	0.8	0.9	0.9	1
19	0.3	0.9	0.9	0.9	1	1	1
21	0.4	1	1	1	1	1	1
23	0.5	0.9	0.9	0.9	0.9	0.9	0.8
Thresholds: 0.5	Calculated VA :	-0.15	-0.14	-0.14	-0.15	-0.14	-0.159
0.6		-0.09	-0.07	-0.06	-0.09	-0.07	-0.08
0.66		-0.05	-0.03	-0.02	-0.06	-0.03	-0.04

Table 1- Data calculated to plot psychometric function.

Calculations similar to those that generated Table 1 were performed for each of the 20 subjects. Each table is used to plot six psychometric functions, one for each noise level. On each psychometric function three levels of threshold of probability of correct answer at 50%, 60% and 66% were applied to find the visual acuity. Results Tables for all subjects can be found in Appendix C.

Root Mean Square Error

To quantify the difference between the values of the model estimated VA and the experimental VA a root mean square error was calculated. This parameter measures the average of the square of the error. The error is obtained by subtracting the estimated VA value from the experimental result Table 2.

The RMS error assesses the quality of the simulation result in terms of its variation. For an unbiased estimator, the RMS error is equal to the standard deviation. Like the standard deviation, the RMS error has the same unit of measurement as the quantity being estimated.

Table 1 shows an example of finding the probability of a correct response of the model while varying the amount of Gaussian white noise. The result is then assessed by finding the RMS error between the experimental VA and the calculated VA.

As could be seen in the Table 1, for each subject 10 letter sizes and 6 noise levels are used. Letter sizes are spaced 0.1 logMAR apart. The portion of correct matching of the test letter with the template letters was calculated.

From the obtained data, the psychometric function was plotted for each noise level. To estimate the subject's visual acuity, three different threshold criteria were examined (threshold criterion of Probability = 0.5, 0.55 and 0.6). Then to choose the best threshold the RMS error between experimental result and computational result was calculated. Table 2 shows an example of the values of RMS error for all thresholds and noise levels for the subject 4 (see Appendix C for all 20 subject's tables).

Noise =		20	40	60	80	100	120
Exp. VA	Thresholds	RMS Error					
6/6 = 0 LogMAR	0.5	0.11	0.10	0.10	0.11	0.10	0.11
	0.6	0.06	0.05	0.04	0.07	0.05	0.06
	0.66	0.03	0.02	0.015*	0.04	0.02	0.03

Table 2- The RMS error between the experimental VA and the calculated VA, for three different thresholds, and six noise levels, for subject 4.

Among all calculated visual acuity RMS errors in Table 2 the value corresponding to the noise level 60 and threshold 0.66 presents the smallest visual acuity RMS error (one example is shown in the Figure 19). Threshold 0.66 was the best choice for all other subjects of this study.

Effect of Different Parameters

Templates

Two types of templates were tested in the model: the original letter images and the aberrated letter images. Based on comparing the average of the calculated VAs and the average of the experimental VAs, the visual acuity approximations when using the images of the aberrated letters as a template were much closer to the experimental results.

This was apparent even when comparing VAs for each subject. Therefore the aberrated letters were chosen as the template for the simulation.

Each subject has his/her own set of templates. Each subject's OTF is used to optically filter the original images to make a set of aberrated image templates (10 different alphabet images at ten different sizes).

Noise Level

The letters presented to subjects are a combination of perfect images and noise in the subjects' memory. This noise was simulated in the model as an additive Gaussian white noise.

The noise level was defined as a percentage of the signal amplitude. The signal was the discrete, finite digital Sloan letter image used in the model. The images were 256*256 pixels with amplitude in the range of 0 to 256. Normalizing the images changes the range to be from 0 to 1. For example, when applied to a normalized image, a noise level of 60 means the maximum value of the absolute amplitude of a pixel of noise is 0.6 (60% of 1), while for an original image the maximum value of the absolute amplitude of a pixel of noise is 154 (60% of 256)

No logical algorithm has been found to estimate the noise level for various observers. For each subject ten levels of noise were tested and the noise level that results in minimum RMS error between experiment and model VA was selected. For some subjects better results were obtained at

higher noise levels, while in other subjects, lower noise levels resulted in better results. There was not any correlation between subject's age and their noise levels. This is shown in Table 3.

Subj#	Selected noise	Subj#	Selected noise
3	60	38	120
4	60	46	80
12	80	47	120
13	80	49	20
14	60	50	80
15	20	53	20
19	120	56	100
28	60	66	20
30	20	87	20
37	60	88	100

Table 3 - Selected best noise for each subject

Figure 19 shows the variation of RMS error for a subject versus noise level. Noise levels 20 to 120 in steps of 20 were used. Noise level of 60 has the smallest RMS error.

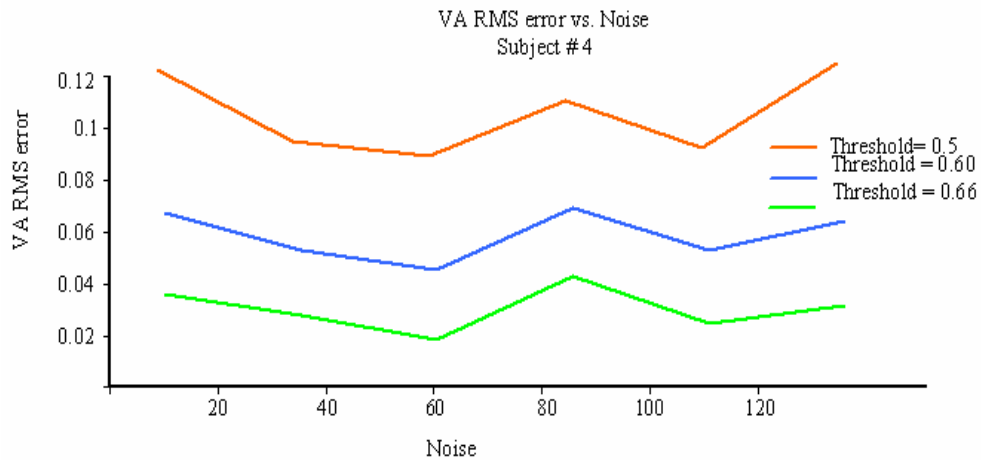


Figure 19: RMS error for subject#4 as a function of noise level.

Frequency Scale

The frequency scale, f , is a parameter used in the equation of the standard contrast sensitivity function. A higher value of the frequency scale shows that the individual can see more details.

Examining three different values for the frequency scale ($f = 0.5, 1, 1.5, \text{ and } 2$) concluded that the best value of visual acuity is calculated at $f = 1$. Therefore, the value of f in all stages of simulation was fixed to one. Figure 20 shows the variation of RMS error vs. the frequency scale.

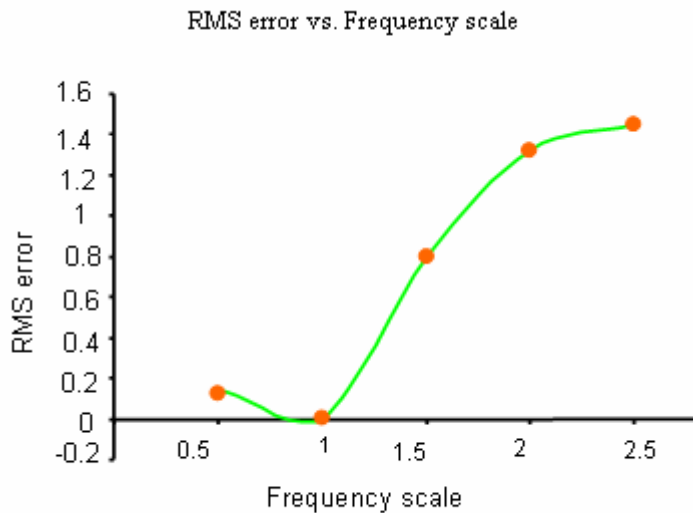


Figure 20: Sample of frequency scale as a function of RMS error for specific subject#28.

Thresholds for Visual Acuity

A visual acuity recognition threshold (the level at which a letter can not only be detected but also recognized) [44] to obtain the model VA results, should be chosen.

For each psychometric function, three values of threshold were tested. The threshold level that resulted in a smaller VA RMS error was selected.

Figure 21 shows the average value of estimated visual acuity using three different thresholds. It can be seen that the estimated VA, for threshold of 0.66, is the closest to the experimental VA. The error is $0.0828 - 0.07357 = 0.0093$.

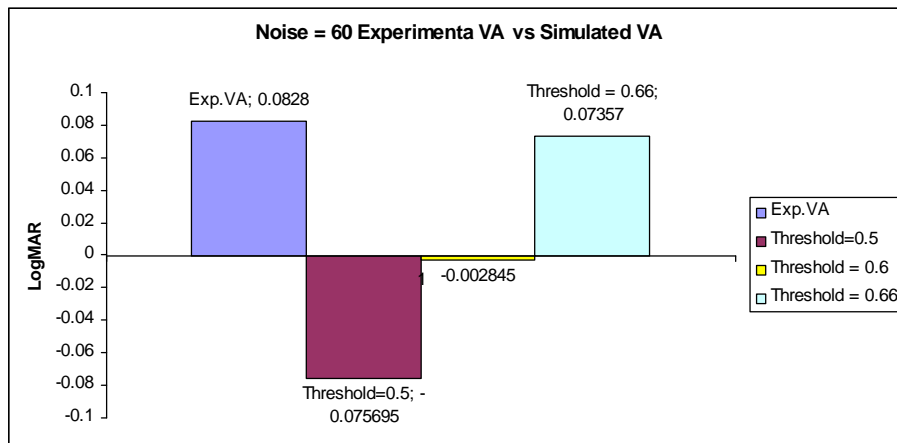


Figure 21: Estimated and experimental average values of visual acuity for 20 subjects.

The plot of RMS error as a function of noise level, Figure 19, also shows that for subject 4 the threshold of 0.66 corresponds to the smallest amount of RMS error, across all noise levels. This holds true for most other subjects as well. Therefore the threshold for VA estimation for this simulation is chosen to be a probability of 66% correct response.

In Figure 22, Figure 23 and Figure 24, visual acuity estimated by the model versus their experimental visual acuity is plotted for 20 subjects for thresholds of 0.66, 0.6, and 0.5. As the P and r (Pearson correlation) values for threshold of 0.66 indicate, these correlation plots emphasize that the 66% threshold is the best choice for the threshold.

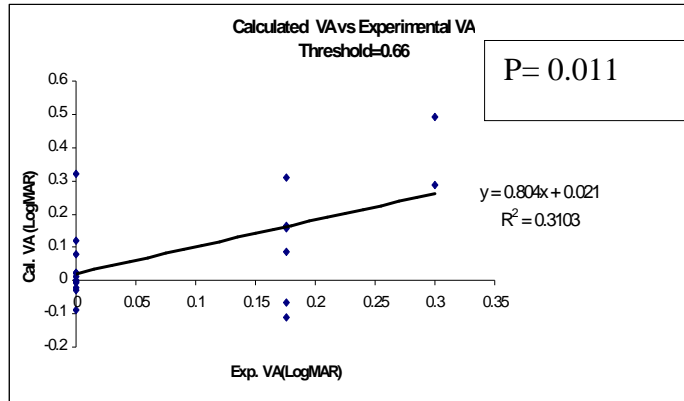


Figure 22: Correlation between Data and Model; Threshold 0.66

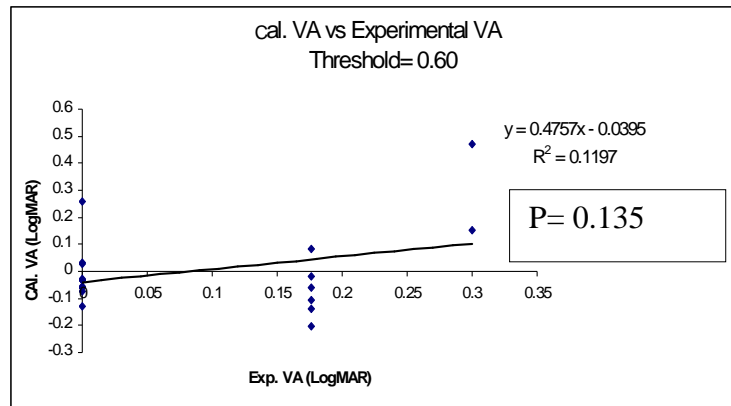


Figure 23: Correlation between Data and Model; Threshold 0.60

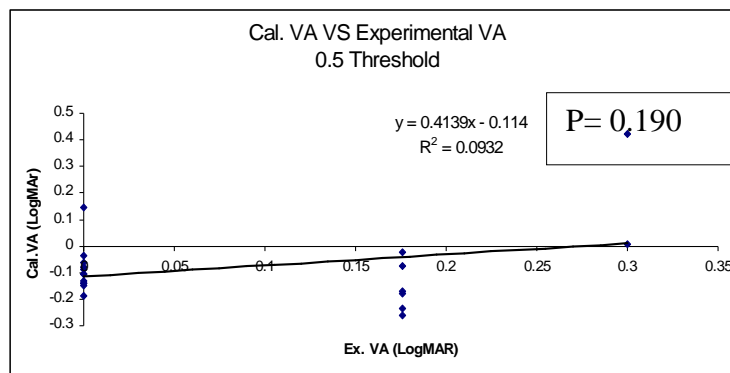


Figure 24: Correlation between Data and Model; Threshold 0.50

Mean Optical Transfer Function

As explained previously, to find the neural filter of the model (Neural Transfer Function) the optical component of Standard Contrast Sensitivity Function (SCSF) should be removed. This optical component is the Mean Optical Transfer Function (MOTF).

Two methods for finding MOTF were examined. In the first method, the average of the OTFs of the 20 subjects was calculated. The NTF was obtained by dividing SCSF by this MOTF. But this technique for finding the NTF did not result in acceptable values for VAs, as the dynamic range of the MOTF was too large (10 to the power of 7).

When MOTF was normalized to a maximum value of 1, its minimum was around 10^{-7} while the same minimum for the MOTF of the second method was around 10^{-3} . As MOTF is in the denominator of the NTF formula, these small values and the large dynamic range caused very large values for NTF and a large dynamic range as well. As shown in Figure 25.

When moving away from the origin (zero) the NTF values drop down at a very high rate. The problem was attempted to be fixed by reducing the dynamic range of the MOTF. The MOTF values less than 10^{-3} were truncated to 10^{-3} . This did not improve the NTF that much.

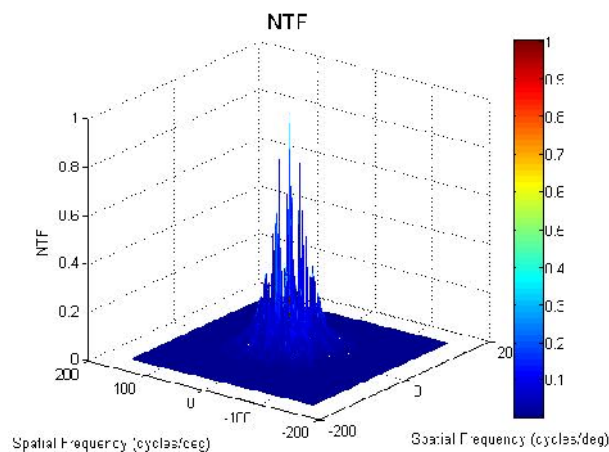


Figure 25: NTF from the first method (MOTF average of OTFs of all the subjects)

In the second method a formula for the MOTF proposed by IJspeert, .et.al was used [43]. This MOTF resulted in very promising estimations for VAs and hence was used in all simulations. Equation (9) shows this MOTF formula. Here, f is the spatial frequency and the age factor is given by (Age Factor = $1 + (\text{age}/70)^4$) (equation(8))

$$\text{MOTF (I, J)} = 1 / (1 + \text{AgeFactor}/7) * (0.426 * \exp(-0.028 * f) + 0.574 * \exp(-0.37 * f)) \\ + 1 / (1 + 7 / \text{AgeFactor}) * (0.125 * \exp(-37 * f) + 0.877 * \exp(-360 * f)) \quad (9)$$

Number of Matching Trials

To find out the probability of a correct response for each letter size, each of the alphabet letters should be compared to all of the other letters of the same size. When this process is done once, each letter is compared to ten template letters. The result of each of these comparisons depends on the effects of the additive noise. Due to the random nature of the additive noise, the same comparison can pass or fail at different trials. To increase the precision of the model each trial can be performed multiple times. When this process is done five times, each letter is compared to fifty template letters that is ten template letters each with five random additive noises.

The results were in the same range as the results from the single trial case.

Figure 26 shows the correlation ($r = 0.721$, $p = 0.279$) between the single trial and the five times repeated trial, for subject 4. Due to the computational complexity and time consuming nature of this process, it was carried out for only five randomly chosen subjects.

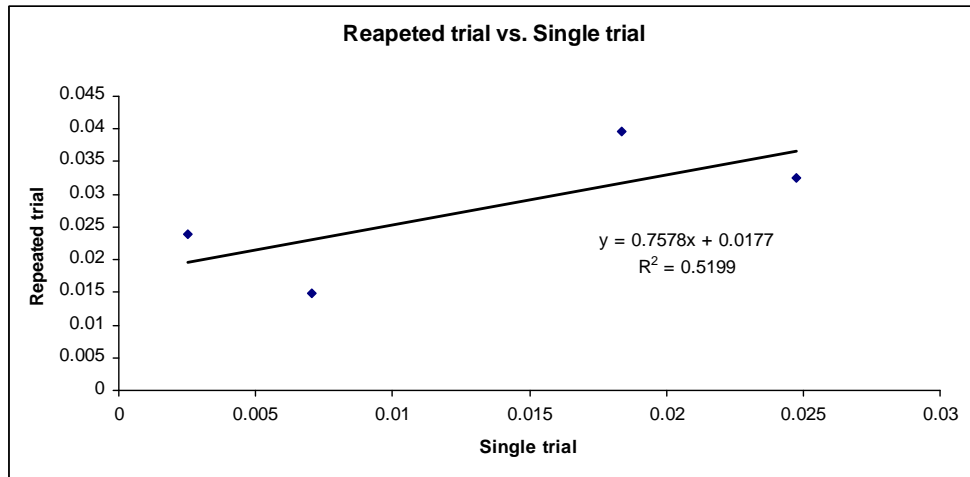


Figure 26: Correlation between 5 time repeating trials vs. Single trial.

Visual Acuity RMS error vs. Different Orders of Aberration

An assumption that was tested was finding if there is any correlation between the RMS values of different orders of aberration and the RMS error of the calculated visual acuity.

In order to test this assumption four experiments were carried out. The correlation between the 2nd order aberrations total RMS and VA RMS error, the correlation between the 3rd order aberrations total RMS and VA RMS error, the correlation between the 4th order aberrations total RMS and VA RMS error, and at last the correlation between the all 15 modes of aberrations total RMS and VA RMS error. Each of these experiments was performed on the twenty subjects.

The results obtained from these correlation calculations as shown in Figure 27 did not reveal any significant relation between VA RMS error and 2nd order aberrations total RMS (defocus and astigmatism). Between these two modes of second order aberrations defocus has more value than astigmatism. Only 2% of the children have greater than 1D of astigmatism. Children's eyes in the experimental data were cyclopedia (paralysis of the ciliary muscle of the eye) so that there was no accommodation of the eye and therefore the actual amount of defocus were obtained. Even though

the defocus and astigmatism terms had different values (one of them small value and the other large) none of them showed any correlation with VA RMS error. There was no significant relation for the 4th order aberrations (spherical aberration) or all 15 modes of aberrations cases either. Despite the fact that children eyes are hyperopic because they have high amplitude of accommodation they can overcome it because of having long range of accommodation compare to adults.

The subjects' VA RMS errors and 3rd order aberrations total RMS (Coma (m=-1, 1) and Trefoil (m=-3, 3)) correlation plots showed P= 0.02, and r = -0.515 which reveals not a very significant but a medium inverse correlation between these two sets of variables. This inverse correlation implies that this model is particularly efficient at estimating the visual acuity of subjects with higher values of 3rd order aberrations total RMS.

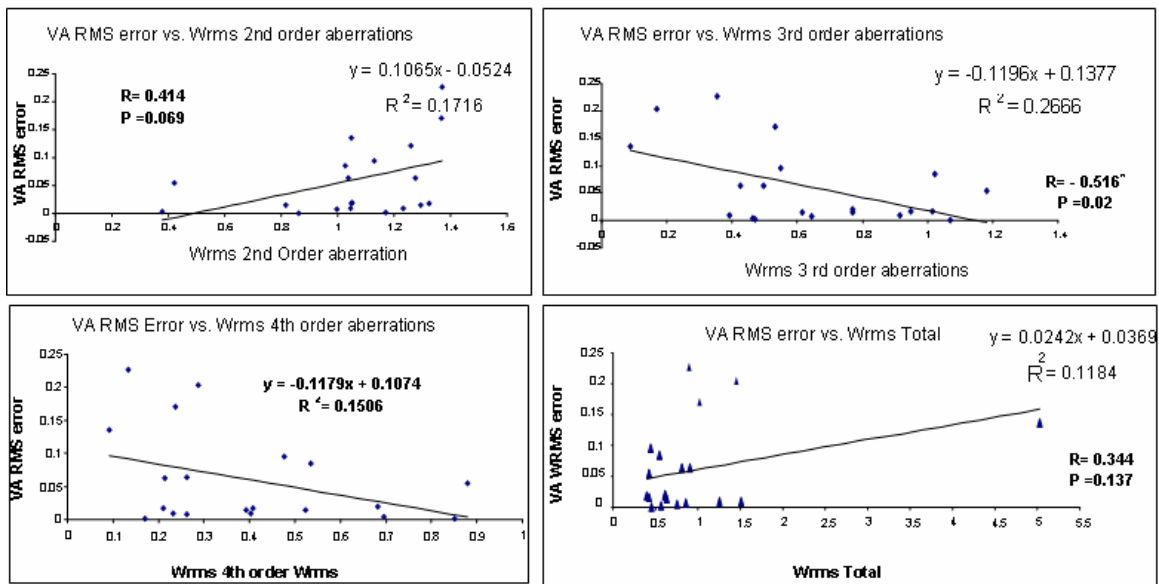


Figure 27: Correlation between 2nd, 3rd, 4th order and total Wrms aberration with VA RMS error.

Chapter 4

Discussion

In this Chapter, I will consider the various parameters and techniques used in this model and will discuss the advantages and disadvantages of the same.

a. Template Matching Algorithm

Several template matching algorithms could be used in the computational model to estimate visual acuity, such as the method of an ideal observer, the minimum distance algorithm, or the normalized correlation [50]. The method used in this model, the normalized correlation, is a widely used pattern matching algorithm [51]. When normalization is used, the effect of the mean value is canceled, and patterns are matched on the basis of shape. MATLAB provides normalized correlation as a predefined function, which simplified the model implementation. As shown in the Results chapter (chapter 3), the template matching algorithm used in this model, performed very well in estimating visual acuity, when using 15 terms of aberrations.

b. Contrast Sensitivity in Children Eyes

The experimental data available were visual acuities of 3 to 6 years old preschool children. Adults and children have similar contrast sensitivity functions; except that the sensitivity of the children is slightly lower than that of adults at all spatial frequencies in this age range [52]. It seems that contrast sensitivity develops quickly in first 3 years of age and then more slowly until it finally reaches adult-like levels at about 9 years of age. The Variability in contrast sensitivity decreases progressively with age [58]. Therefore although the SCSF used in this model was obtained based on adult experimental data it worked quiet well for children as well, as all stages of the model used normalized values.

The other interesting point in development of contrast sensitivity functions is that its development during the “toddler” years has relatively greater improvements at the higher spatial frequencies but after 4 yr of age appears to be mainly improvement at the lower spatial frequencies [58]. For example, from 4 yr of age until maturity, CS improves by about 0.27 log units at the two lowest spatial frequencies, but only by about half of that value (~0.14 log units) at the two highest SF. The frequency scale (), the parameter responsible for varying CSF, was set to 1 for all subjects. Changing to 0.5, 1.5, 2 and 2.5, did not present any improvement on the result of the calculated VA, as shown in Figure 20. Therefore a constant value of contrast sensitivity function was used for all the subjects.

c. Alternative Single Valued Metric

One purpose of implementing this computational model was to find an alternative reliable metric instead of RMS wavefront error to quantify the effects of aberrations on the acuity task. In the case of high values of eye aberrations, RMS wavefront error is a good predictor of visual acuity but when RMS wavefront error is less than 0.25 μm , it is no longer a reliable metric of acuity. This model provides an alternative metric of acuity [38]. This model has shown to be a good predictor of visual acuity as it incorporates the effects of each individual aberration coefficient rather than relying on the RMS wavefront error.

d. Visual Acuity of Preschool Children

There is no universally accepted standard format for finding visual acuity in children. A variety of methods have been proposed by different researchers [53, 54]. For example, the drawing method in which a series of test characters of visual acuity chart are shown to a child and the child is asked to make copies of what he sees using the provided paper and pencil [52].

The other method is the block selection method in which cut-out wooden blocks, the same shape as the test letters, are set before the child, and the child is asked to select a block that matches the picture letter shown [53].

There are a number of more new optotype matching tests that Saunders explained in her book [59]. In her tests all correct responses of child are praised to encourage the child to continue with testing and maintain co-operation. Some acuity tests that are designed for younger children use familiar pictures as targets rather than letters. Some times the child loose interest to answer correctly therefore it is important to know whether failure to match is due to lack of interest or acuity limitations [59].

Different types of children visual acuity are: The Kay Picture test, Allen cards, Fooks symbols, tumbling E test, Lighthouse test, LH symbols, Siiigren's hand test... [59].

In the method that provided the experimental VA data for this model, Cambridge Uncrowded Cards were shown to children and most of the visual acuities found were 6/6. There were a few children with 6/9 or 6/12 VAs (Courtesy of Dr. Bobier's lab).

The experimental data available for this research was restricted to a visual acuity range from 6/6 to 6/12 and age range from 3 to 6 years old. In addition the step sizes changes were larger than the typical of LogMAR. Fortunately these limitations do not have any effects on reliability of the computational results. The only effect was on value of correlation obtained between experimental and computational VA.

This model is similar to that proposed by Watson and Ahumada [7]. Their simulation results had a correlation of over 0.86 with the experimental data of 67 subjects with only two nonzero terms of aberrations (second and forth orders aberration terms), and visual acuities in the range of -0.3 to 0.4 LogMAR. This model has a correlation of 0.56 with the experimental data of 20 subjects with 15 terms of aberrations. The lower correlation could be due to the higher number of aberration terms (15 vs. 2) or the limited distribution of the visual acuity of the subjects from the experimental data.

e. Effects of Noise

This research attempted to find an algorithm to estimate the noise level of each subject's visual system. It is unclear which neural stage is critical in the observer's performance in letter identification. It seems behavior of neurons responsible for the noise follows probabilistic distributions that can be roughly approximated [55]. A better understanding of the role of spatial frequency channels in human letter identification, could guide one in the finding of a rule for determining exact values for the noise level of each individual's visual system.

For some subjects increasing the noise makes the VA results better, showing that adding some noise to a weak signal can improve signal detection (one can think of this as a case of stochastic resonance). The model demonstrated that each observer has a different estimate of the best noise level. Perhaps it is not very surprising to know that the subjects should be differing in this aspect, having for example, variations in their retinal cone density, or ganglion cell connectivity, etc. [48].

f. Effects of Infra Red vs. Visible Light on VA

Zernike expansions of the experimental wave-front aberration functions were used to determine aberration coefficients. These aberration coefficients, obtained from images of the subject's eye, were used to find the optical filter (OTF) of the model and ultimately to estimate the VA. The wavelength of the light used to get the images of the eyes was 780 nm, which is in the near infrared region of the electromagnetic spectrum.

Finding the experimental visual acuity of the individuals was carried out under visible light with wavelengths from 400 to 700 nm.

Using infrared light, for which the eye has relatively low efficiency compared to the visible light, might be the reason that the simulated VAs were mostly better than the experimental VAs.

As is well known, newborn infants are hyperopic, and a process of emmetropization occurs as the child gets older [57]. Most of the subjects for whom data were available had moderate hyperopia (~ 3.00 diopters).

g. Different MOTFs

Even though using the average of the Optical Transfer Functions (OTF) of all the subjects as the MOTF sounds rational, but it did not give an acceptable estimation for the MOTF.

A third method that could be used (not examined in this study) for estimating the MOTF is to calculate the average of all the subjects wavefront aberrations terms, and use the resulting 15 terms to calculate the OTF to be used as the estimation for the MOTF.

h. Using Adaptive Procedures in Template Matching

To improve the speed and accuracy of the template matching model, an adaptive procedure can be applied to the size selection at each trial [49]. Instead of testing all the letters of each of the ten sizes, the test size of the next trial would be based on the percentage of correct answers of the previous one or more sizes.

For example if the percentage of correct answers for letter size of 0 LogMAR is 80% the next trial would test letter size -0.3 LogMAR, but if the percentage of correct answers for letter size of 0 LogMAR is 40% the next trial would test letter size 0.3 LogMAR.

i. Running the Simulation on a Larger Population

Statistically it is likely that having more degrees of freedom would give more accurate results. Therefore it is expected that running the model on more than twenty subjects with a variety of VAs (and not just 6/6, 6/9 and 6/12) and more age variation as well could result in a higher level of correlation between calculated VAs and experimental VAs. On the other hand simulating the

model for 20 subjects needed three computers to run for 10 hours. Therefore first the speed improvement for running the model should be obtained.

Analyzing the output raw data and plotting of the psychometric functions to calculate the VAs took at least twice as much time. The model can be optimized for speed. A faster computational algorithm (or faster processors) would make simulations for more subjects possible.

It can be concluded that a variety of factors were contributing to the outcome of the calculations, with the three main factors being:

The Optimum noise level for each observer.

Accuracy and range of VAs of the experimental data.

The MOTF used for calculating the neural filter.

Conclusion

The model presented in this research makes it possible to find visual acuity in people whose visual acuity can not be measured subjectively. For example preschool children, individual whose mental development are relatively slow, non-verbal individuals or anyone who cannot read the English alphabet on VA letter charts.

The RMS error obtained using this model was about 0.01 LogMAR. The small value of the error means that this model is able to estimate visual acuity from the 15 terms of aberrations. The model can also determine the effect of removing one or more of the aberration terms on the visual acuity. An application of the model is to predict the effects of laser correction of one or more aberration terms on visual acuity. This will be subject for future study.

Appendices

Appendix A

MATLAB Simulation Codes

Main.m

The following parameters are defined in the “Parameters to Change” section:

Subject numbers (goodSubjects)

Type of MOTF used (motfType)

Type of Template used (templateType)

Then MOTF , and NTF are calculated.

Next for each subject WA, PSF and OTF are calculated and for 10 sizes the templates are created, then for 6 noise levels, each of the 10 letters are filtered and compared with the templates, probability corrects are calculated, and the result is saved in an excel file.

```
clear; close all; clc;

%%%%%%%%%%%%%%%%%%%%%%%%%%%%%%%%%%%%%%%%%%%%%%%%%%%%%%%%%%%%%%%%%%%%%%%%
% P A R A M E T E R S   T O   C H A N G E
%%%%%%%%%%%%%%%%%%%%%%%%%%%%%%%%%%%%%%%%%%%%%%%%%%%%%%%%%%%%%%%%%%%%%%%%
goodSubjects = [3  4 12 13 14 15   19 28 47 49 50 53   37 38 56 87 46 30   66 88];

motfType = 1;           % 0: avg90,    1: Ahumada
templateType = 1;      % 0: original, 1: retinal
%%%%%%%%%%%%%%%%%%%%%%%%%%%%%%%%%%%%%%%%%%%%%%%%%%%%%%%%%%%%%%%%%%%%%%%%
sizeValues = [5 7 9 11 13 15 17 19 21 23 ];
noise = [0 0 20 40 60 80 100 120];    % IMPORTANT: keep 0, is place holder for Wrms js
visActThreshold = [0.5, 0.6, 0.66];
%%%%%%%%%%%%%%%%%%%%%%%%%%%%%%%%%%%%%%%%%%%%%%%%%%%%%%%%%%%%%%%%%%%%%%%%

sizePad = zeros(1,27);
for i = 1:length(sizeValues)
sizePad (1, i) = sizeValues (1, i);
end

result (2, 6:8) = visActThreshold(1:3);
result (2, 10:36) = sizePad (1, 1:27);

if (motfType == 0)
disp('Creating NTF ... from avg90(OTF)');
MOTF = make_MOTF_avg90;
```

```

NTF = make_NTF(MOTF);
else
disp('Creating NTF ... from Ahumada MOTF');
MOTF = make_MOTF;
NTF = make_NTF(MOTF);
end

for cnt_subj = 1:length(goodSubjects);
subjNum = goodSubjects(cnt_subj);

disp(['SubjNum = ', int2str(subjNum)]);

disp('Initializing ...');
[Wrmsj, xw, yw, jmax, dw, P, apw, lambda] = make_initials(subjNum);

disp('Creating WA ...');
W = make_WA(Wrmsj, xw, yw, jmax, dw);

disp('Creating PSF ...');
PSF = make_PSF(P, apw, W, lambda);

disp('Creating OTF ...');
OTF = make_OTF(PSF);

if (templateType == 0)
disp('Original letter Template ...');
else
disp('Retinal Template ...');
end

prob = zeros(length(noise), 27);
correct(1:27) = 0;
numberOfLetters = 10;

disp('Sampling ...');

for cnt_size = 1:length(sizeValues);
letterSize = sizeValues(cnt_size);
template_spat = make_template(letterSize, OTF, templateType);

result ((subjNum*length(noise))+1, 1) = subjNum;
result ((subjNum*length(noise))+1, 4:15) = Wrmsj(4:15)*1000;

for cnt_noise = 2:length(noise);
noiseScale = noise(cnt_noise);

disp(['Noise = ', int2str(noiseScale)]);

for letterNumber = 1:numberOfLetters; % 1C 2D 3H 4K 5N 6O 7R 8S 9V 10Z
noised_spat = filter_freqDomain(letterNumber, letterSize, OTF, NTF, noiseScale);
correctness = match_normxcorr2(letterSize, letterNumber, noised_spat, template_spat);
correct(letterNumber) = correctness;
prob(cnt_noise, cnt_size) = prob(cnt_noise, cnt_size) + correctness;
end
disp(['Size = ', int2str(letterSize), ' correct = ', int2str(correct(1)),
int2str(correct(2)), int2str(correct(3)), int2str(correct(4)), int2str(correct(5)),
int2str(correct(6)), int2str(correct(7)), int2str(correct(8)), int2str(correct(9)),
int2str(correct(10))]);

result ((subjNum*length(noise))+cnt_noise, 1) = subjNum;
result ((subjNum*length(noise))+cnt_noise, 2) = noiseScale;

```

```

result ((subjNum*length(noise))+cnt_noise, 3) = motfType;
result ((subjNum*length(noise))+cnt_noise, 4) = templateType;

prob(cnt_noise, cnt_size) = prob(cnt_noise, cnt_size) / numberOfLetters;
end

row = (subjNum*length(noise))+2;
result (row:(row+length(noise)-2), 10:36) = prob(2:length(noise), 1:27);
end

xlswrite ('resultSubj12Size10Noise5_0_20.xls', result);
end

disp('End!');

```

make_initials.m

```

function [Wrmsj, xw, yw, jmax, dw, P, apw, lambda] = make_initials (subjNum)

d = 5;
expZer = xlsread('90Subj_Normalized.xls', 'a1:o90');

Wrmsj = expZer(subjNum, :);
jmax = length(Wrmsj)-1;
lambda = 780;

Wrmst = 0;
for j=0:jmax
Wrmst=Wrmst+Wrmsj(j+1)^2;
end
Wrmsttotal=sqrt(Wrmst); %total rms wavefront error in um

% =====
% Convert units for calculation

Wrmsj=Wrmsj*1e-3; %rms wavefront error coefficients in mm
Wrmsttotal=Wrmsttotal*1e-3; %total rms wavefront error in mm

lambda=lambda*1e-6; %wavelength in mm
dw=d/lambda; %pupil diameter in number of wavelengths
PRw=0.5*dw; %pupil radius in number of wavelengths
apw=pi*PRw^2; %pupil area in wavelength^2

% =====

%rsh 1 pixel = 0.00318 deg ==> 1 pixel = 70.42 lambda ==>
%rsh lambda = 570 ==> 1 pixel = 0.040 mm ==> 5 mm = 125 pixel
%rsh lambda = 780 ==> 1 pixel = 0.055 mm ==> 5 mm = 91 pixel
pixel = round( 5 / (70.42 * lambda) );
xylimit = PRw;
dxyw = PRw*2/pixel; %x-coordinate pixel width in number of wavelengths

xywmin = -xylimit; %minimum x-coordinate in number of wavelengths
xywmax = xylimit; %maximum x-coordinate in number of wavelengths

```

```

xw=xywmin:dxyw:xywmax;    %x-coordinates in number of wavelengths
yw=xw;    %y-coordinates in number of wavelengths
size(xw);
Imax=length(xw);
Jmax=length(yw);

% Set-up circular pupil
for I=1:Imax
for J=1:Jmax
P(I,J)=(sqrt(xw(I)^2+yw(J)^2) <= PRw);
end
end

```

Make_WA.m

```

function W = make_WA(Wrmsj, xw, yw, jmax, dw)

W=zeros(length(xw),length(yw));
for j=0:jmax
n=ceil((-3+sqrt(9+8*j))/2);    %highest power or order of the radial polynomial term
m=2*j-n*(n+2);                %azimuthal frequency of the sinusoidal component
W=W+Wrmsj(j+1)*zernike(n,m,xw,yw,dw);
end

```

Zernike.m

```

function Znm=zernike(n,m,x,y,d)

% zernike.m is a function that computes the values of a Zernike Polynomial
%           over a circular pupil of diameter d
% Output:
% Znm is the Zernike polynomial term of order n and frequency m

%Input:
% n = highest power or order of the radial polynomial term, [a positive integer]
% m = azimuthal frequency of the sinusoidal component, [a signed integer, |m| <= n]
% x = 1-D array of pupil x-coordinate values, [length(x) must equal length(y)]
% y = 1-D array of pupil y-coordinate values, [length(y) must equal length(x)]
% d = pupil diameter
%%%%%%%%%%%%%%%%%%%%%%%%%%%%%%%%%%%%%%%%%%%%%%%%%%%%%%%%%%%%%%%%%%%%%%%%
% initialize circular pupil function
%%%%%%%%%%%%%%%%%%%%%%%%%%%%%%%%%%%%%%%%%%%%%%%%%%%%%%%%%%%%%%%%%%%%%%%%

Imax=length(x);
Jmax=length(y);
a=d/2;

for I=1:Imax    %initialize circular pupil
for J=1:Jmax

```

```

p(I,J)=(sqrt(x(I)^2+y(J)^2) <= a);
end
end

%%%%%%%%%%%%%%%%%%%%%%%%%%%%%%%%%%%%%%%%%%%%%%%%%%%%%%%%%%%%%%%%%%%%%%%%
% Compute Normalization Constant
%%%%%%%%%%%%%%%%%%%%%%%%%%%%%%%%%%%%%%%%%%%%%%%%%%%%%%%%%%%%%%%%%%%%%%%%

Nnm=sqrt(2*(n+1)/(1+(m==0)));

Zj = ((n*(n+2))+m)/2;
nnn = length(x);

%%%%%%%%%%%%%%%%%%%%%%%%%%%%%%%%%%%%%%%%%%%%%%%%%%%%%%%%%%%%%%%%%%%%%%%%
% Compute Zernike polynomial
%%%%%%%%%%%%%%%%%%%%%%%%%%%%%%%%%%%%%%%%%%%%%%%%%%%%%%%%%%%%%%%%%%%%%%%%
%
% if n==0
%   Znm=p;
% else
%   Znm=zeros(Imax,Jmax);
%   for I=1:Imax
%     for J=1:Jmax
%       r=sqrt(x(I)^2+y(J)^2);
%       if (x(I)>=0 && y(J)>=0) || (x(I)>=0 && y(J)<0)
%         theta=atan(y(J)/(x(I)+1e-20));
%       else
%         theta=pi+atan(y(J)/(x(I)+1e-20));
%       end
%       for s=0:0.5*(n-abs(m))
%         Znm(I,J)=Znm(I,J)+(-1)^s*factorial(n-s)*(r/a)^(n-2*s)/(factorial(s)*...
%           factorial(0.5*(n+abs(m))-s)*factorial(0.5*(n-abs(m))-s));
%       end
%       Znm(I,J)=p(I,J)*Nnm*Znm(I,J)*((m>=0)*cos(m*theta)-(m<0)*sin(m*theta));
%     end
%   end
% end
%
%
% disp(['Saving Zernike ...', int2str(nnn)]);
% ZerWFid=fopen(['Zer_j_',int2str(Zj),'_',int2str(nnn),'.zer'],'w');
% count = fwrite(ZerWFid, Znm, 'float64')
% fclose('all');
%
%
% disp(['Reading Zernike ...', int2str(nnn)]);
ZerRFid=fopen(['Zer_j_',int2str(Zj),'_',int2str(nnn),'.zer'],'r');
Znm = fread(ZerRFid,'float64');
fclose('all');
Znm = reshape(Znm, nnn, nnn);

```

Make_PSF.m

```

function PSF = make_PSF(P, apw, W, lambda)
sizeP = size(P)
npadding = (256 - sizeP(1))/2;

P2 = padarray(P,[npadding,npadding]);

```

```

W2 = padarray(W,[npadding,npadding]);

PSF=fft2((P2.*exp(-i*2*pi*W2/lambda)))/apw;
PSF=fftshift(PSF);
PSF=PSF.*conj(PSF);
PSF=rot90(PSF);
PSF=flipud(PSF);
PSF=PSF/max(max(PSF)); % Normalize PSF

```

Make_OTF.m

```

function OTF = make_OTF(PSF)
OTF=fft2(PSF);
OTF=OTF/max(max(OTF));
OTF=fftshift(OTF);
OTF=rot90(OTF);
OTF=flipud(OTF);

```

Make_CSF.m

```

function SCSF = make_CSF
f0 = 4.1726;
f1 = 1.3625;
a = 0.8493;
p = 0.7786;
phi = 1; % phi (frequency scale) manually set equal to 1

% test peak values
fmax = 3.45;
Gain = 373.08;
maximum = Gain*(sech((fmax/(phi*f0))^p) - a*sech(fmax/(phi*f1)));

%M = 0.0142, N=18017.5
%1 pixel = 70.3809 cyc/rad
%1 pixel = 1.2283 cyc/deg
%256 pixels = 314.4448 cyc/deg
xyflim=157.2224; %minimum xf-coordinate in degree/cycle
dxyf=xyflim/127.5; %xf-coordinate pixel width in number of frequencies
xf = -xyflim:dxyf:xyflim; %x-coordinates in number of frequencies
yf = -xyflim:dxyf:xyflim; %y-coordinates in number of frequencies
size(yf);
Imax=length(xf);
Jmax=length(yf);

SCSF = zeros(Imax, Jmax);

for I=1:Imax
for J=1:Jmax
f = sqrt(xf(I)^2+yf(J)^2);
SCSF(I,J) = Gain*(sech((f/(phi*f0))^p) - a*sech(f/(phi*f1)));
end
end

```

```
SCSF = SCSF/max(max(SCSF));
```

Make_MOTF.m

```
function MOTF = make_MOTF;
age = 35;
D = 70;

%M = 0.0142, N=18017.5
%1 pixel = 70.3809 cyc/rad
%1 pixel = 1.2283 cyc/deg
%256 pixels = 314.4448 cyc/deg
xyflim=157.2224; %minimum xf-coordinate in degree/cycle
dxyf=xyflim/127.5; %xf-coordinate pixel width in number of frequencies
xf = -xyflim:dxyf:xyflim; %x-coordinates in number of frequencies
yf = -xyflim:dxyf:xyflim; %y-coordinates in number of frequencies
size(yf);
Imax=length(xf);
Jmax=length(yf);

MOTF = zeros(Imax, Jmax);

ageFactor = 1 + (age/D)^4;
for I=1:Imax
for J=1:Jmax
f = sqrt(xf(I)^2+yf(J)^2);
MOTF(I,J) = 1/(1+ageFactor/7)*(0.426*exp(-0.028*f)+0.574*exp(-0.37*f)) +
1/(1+7/ageFactor)*(0.125*exp(-37*f)+0.877*exp(-360*f));
end
end

MOTF = MOTF/max(max(MOTF));
```

Make_MOTF_avg90.m

```
function MOTF = make_MOTF_avg90

% numberOfSubjects = 90;
%
% MOTF = zeros(256);
%
% for subjCnt = 1:numberOfSubjects
%
% disp('Initializing ...');
% [Wrmsj, xw, yw, jmax, dw, P, apw, lambda] = make_initials(subjCnt);
%
% disp('Creating WA ...');
% W = make_WA(Wrmsj, xw, yw, jmax, dw);
%
% disp('Creating PSF ...');
% PSF = make_PSF(P, apw, W, lambda);
```

```

%
% disp('Creating OTF ...');
% OTF = make_OTF(PSF);
%
% MOTF = MOTF + OTF;
%
% end
%
% MOTF = MOTF / numberOfSubjects;
%
% this is to reduce the dynamic range of MOTF which is 10^20 or so
% MOTF = abs(MOTF);
% MOTF = MOTF / max(max(MOTF));
% MOTF = (MOTF>=0.001) .* MOTF;
% MOTF = MOTF + 0.001;

% disp('Saving MOTF avg90 ...');
% MotfWfFid=fopen('MotfAvg90.aza','w');
% count = fwrite(MotfWfFid, MOTF, 'float64');
% fclose('all');

disp('Reading MOTF avg90 ...');
MotfRFid=fopen('MotfAvg90.aza','r');
MOTF = fread(MotfRFid,'float64');
fclose('all');
MOTF = reshape(MOTF, 256, 256);

```

Make_NTF.m

```

function NTF = make_NTF(MOTF)
SCSF = make_CSF;
NTF = SCSF ./ MOTF;
NTF = NTF / max(max(NTF));           % normalizing NTF to its max
Imageread_LetterMatrix.m
function letter_image = imageread_LettMatrx(num_let, num_size)
imfid =
fopen(['LettMatrix/Num',int2str(num_let),'_Size',int2str(num_size),'.Lett'],'r');
letter_image = fread(imfid);
fclose('all');
letter_image = reshape(letter_image, 256, 256);

filter_frequencyDomain.m
function noised_spat = filter_freqDomain(num_let, num_size, OTF, NTF, noise_scale)

letter_spat = imageread_LettMatrx(num_let, num_size);

scale = 2^8;
scale_image = (1/4);

retinal_freq = fft2(letter_spat) .* OTF;
retinal_spat = abs(ifftshift(ifft2(retinal_freq)));
retinal_spat = retinal_spat*scale/max(max(retinal_spat));

neural_freq = retinal_freq .* NTF;
neural_spat = abs(ifftshift(ifft2(neural_freq)));
neural_spat = neural_spat*scale/max(max(neural_spat));

noisedB = 1;
whiteGN = wgn(size(neural_spat,1),size(neural_spat,2),noisedB);

```

```
noised_spat = neural_spat + whiteGN*noise_scale/100*scale/max(max(whiteGN));
```

Make_template.m

```
function template_spat = make_template(num_size, OTF, templateType)
%if templateType is 0:original, do NOT do OTF
%if templateType is 1:retinal, do OTF
for num_let=1:10
letter_spat = imageread_LettMatrx(num_let, num_size);
retinal_spat = letter_spat;

if (templateType == 1) % if retinal, do OTF
retinal_freq = fft2(letter_spat) .* OTF;
retinal_spat = abs(ifftshift(ifft2(retinal_freq)));
end
template_spat(:,:,num_let) = retinal_spat/max(max(retinal_spat)) * 2^8;
end
```

match_normxcorr2.m

```
function correctness = match_normxcorr2(num_size, num_let, noised_spat, template_spat)

discriminant=zeros(1, 10);

for i=1:10
cc = normxcorr2(template_spat(:,:,i), noised_spat);
discriminant(i) = max(max(cc));
end

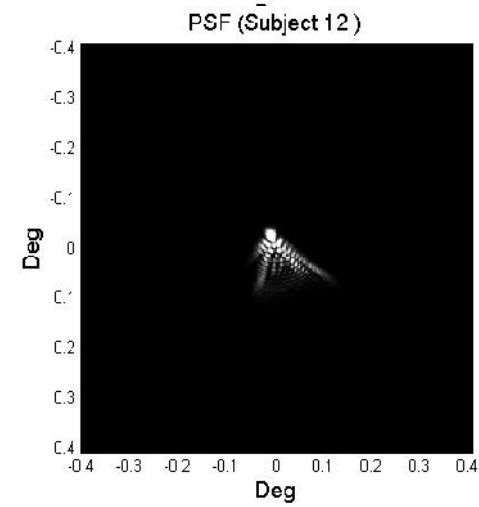
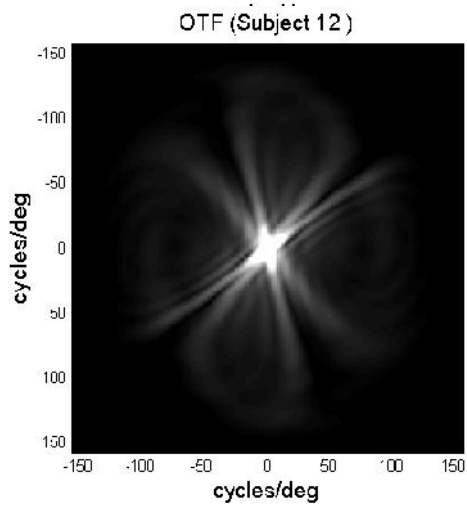
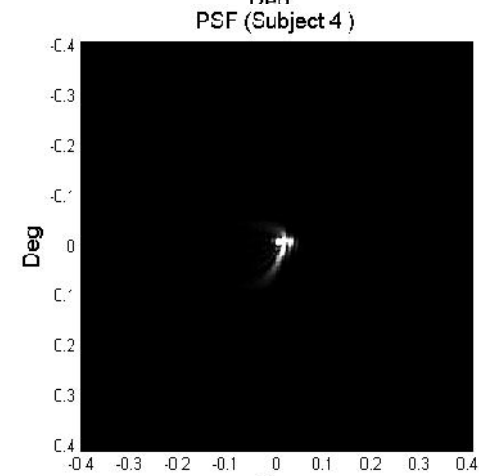
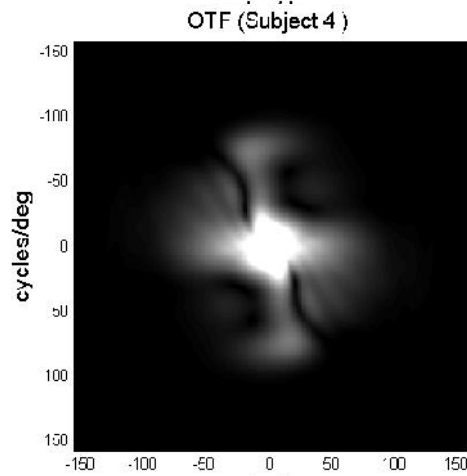
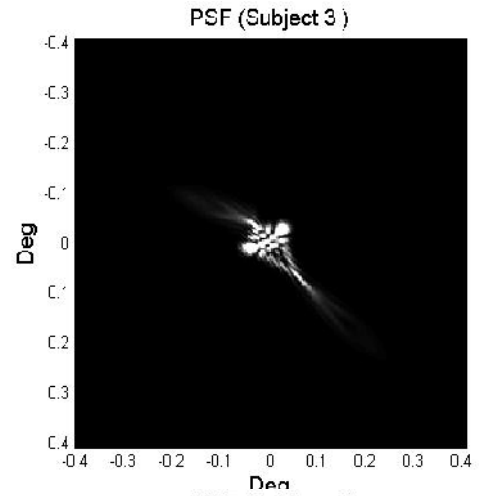
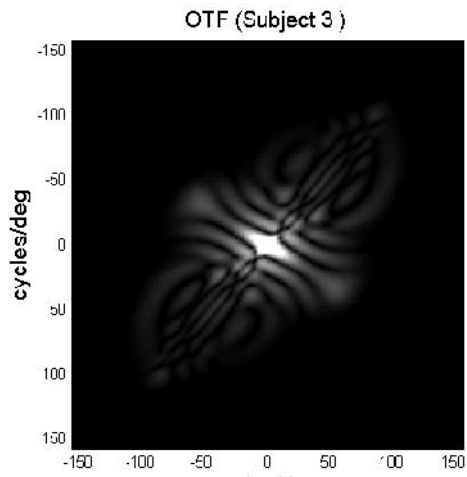
[max_discriminant, num_lett_matched] = max(discriminant);

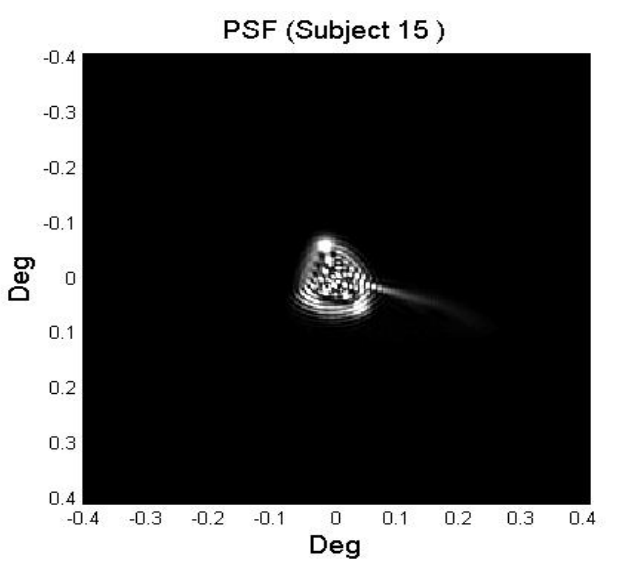
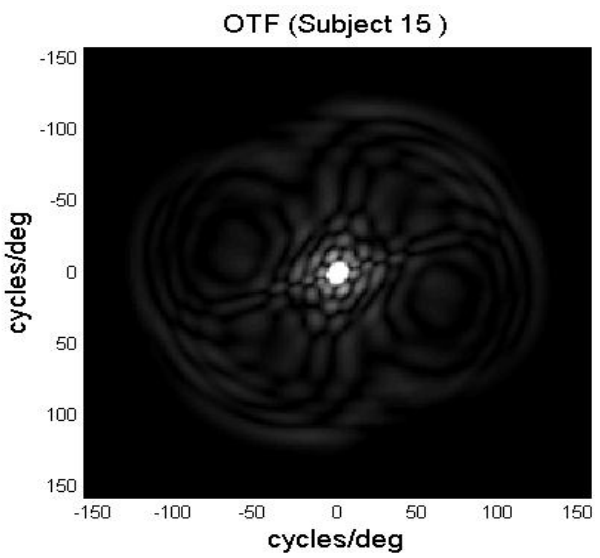
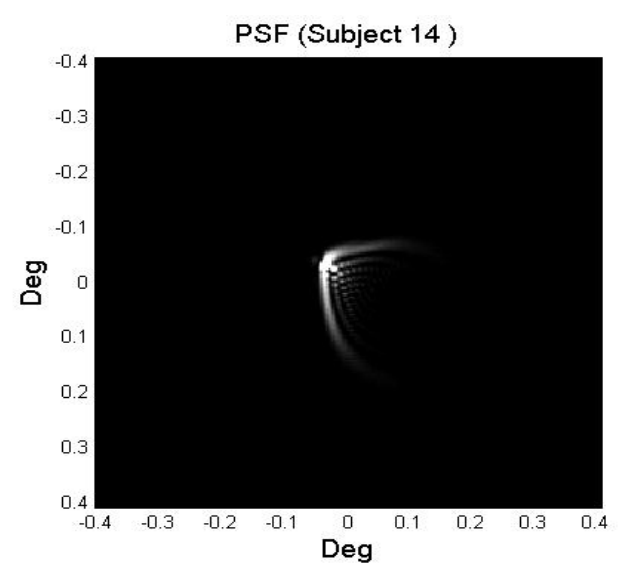
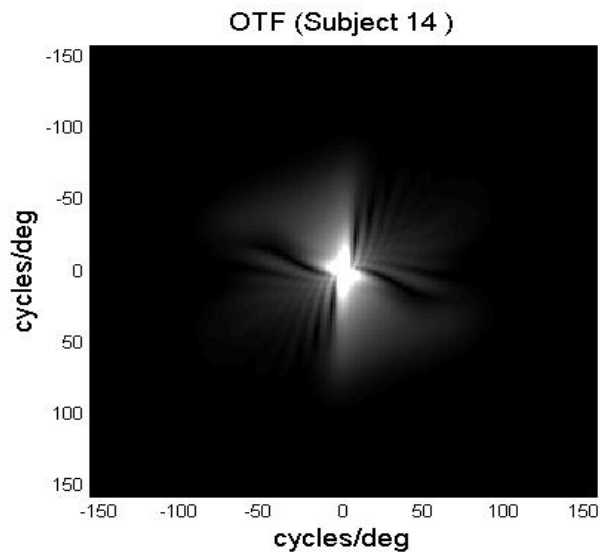
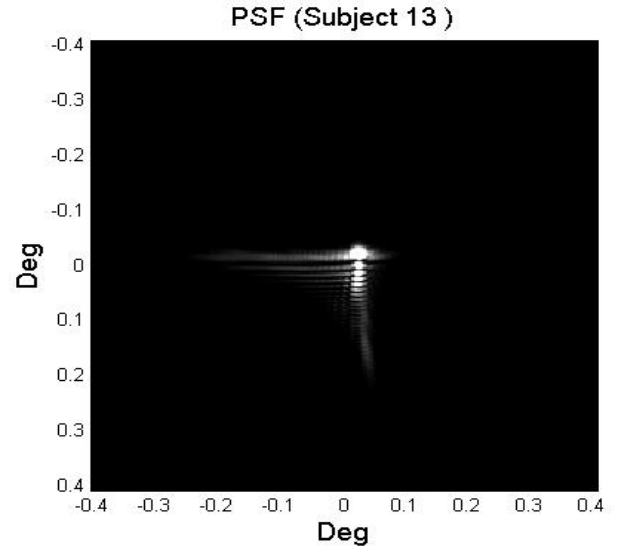
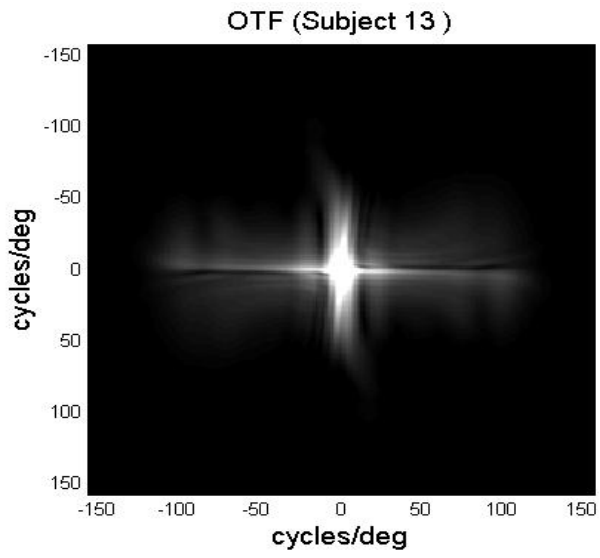
matched_image = imageread_LettMatrx(num_lett_matched, num_size);

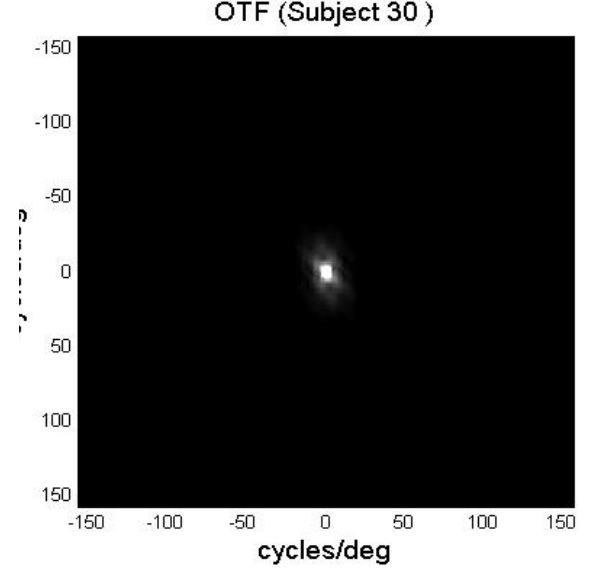
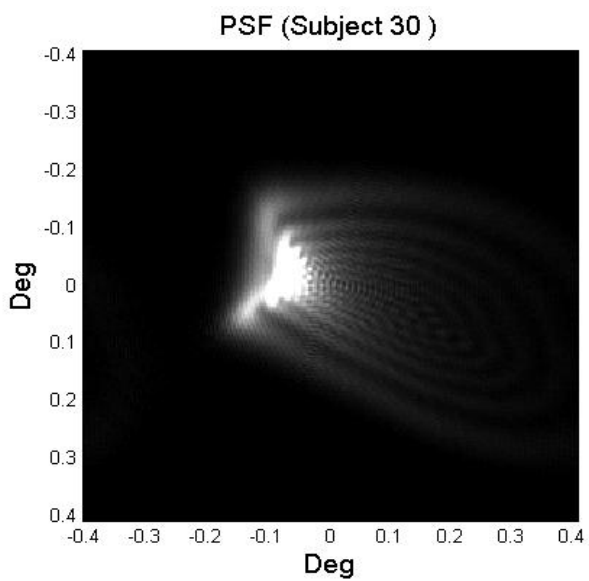
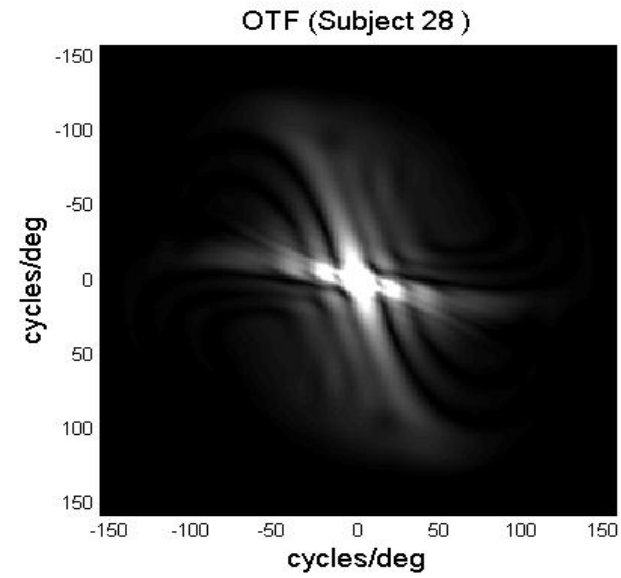
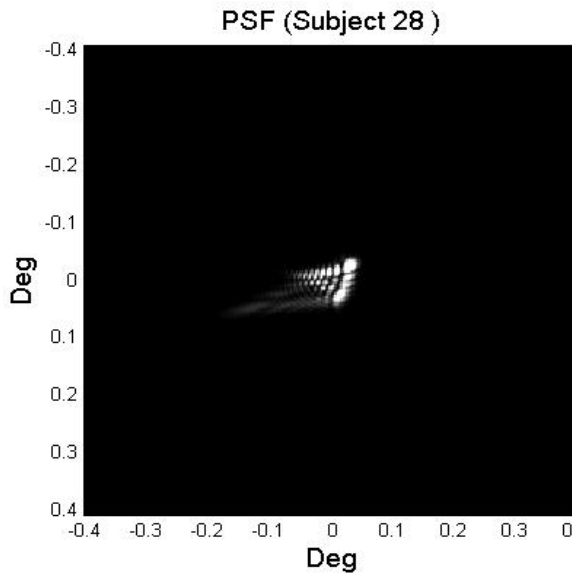
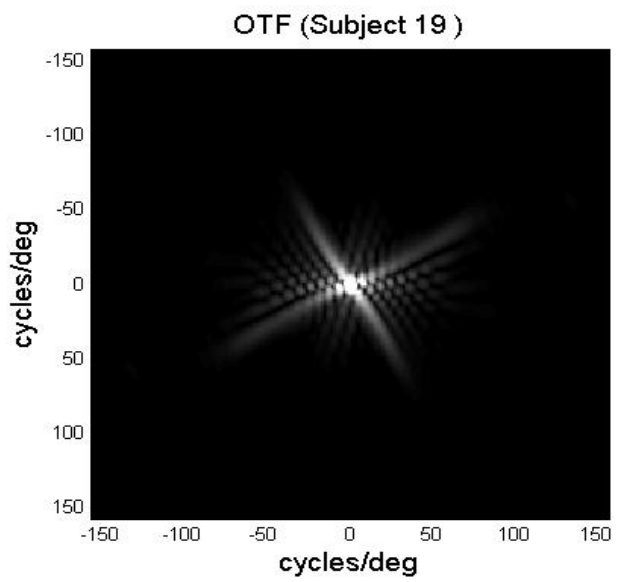
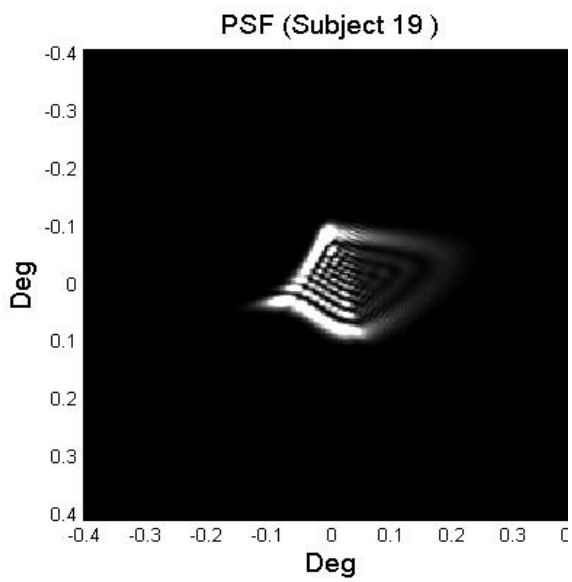
if (num_lett_matched == num_let)
correctness = 1;
else
correctness = 0;
end
```

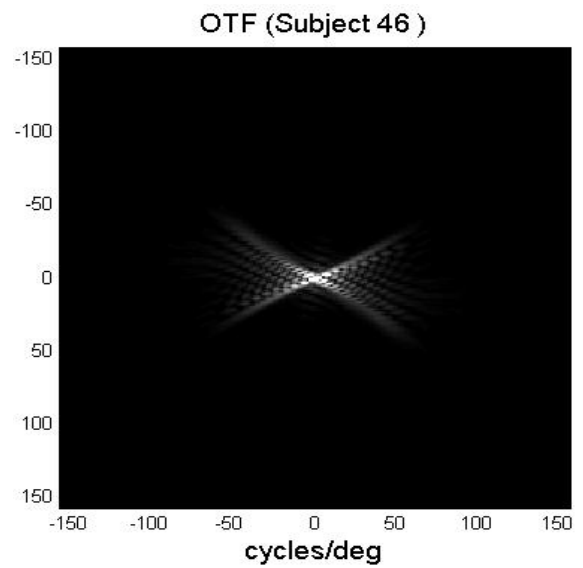
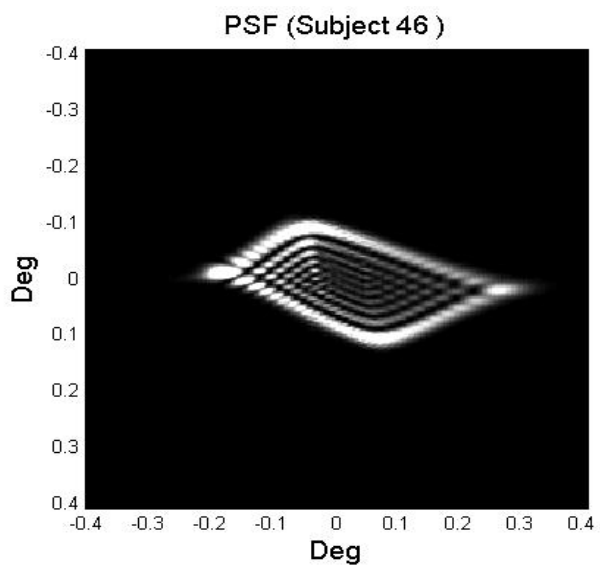
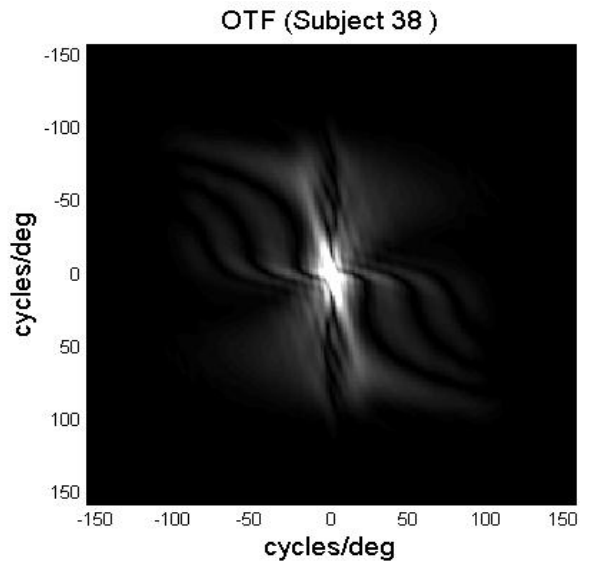
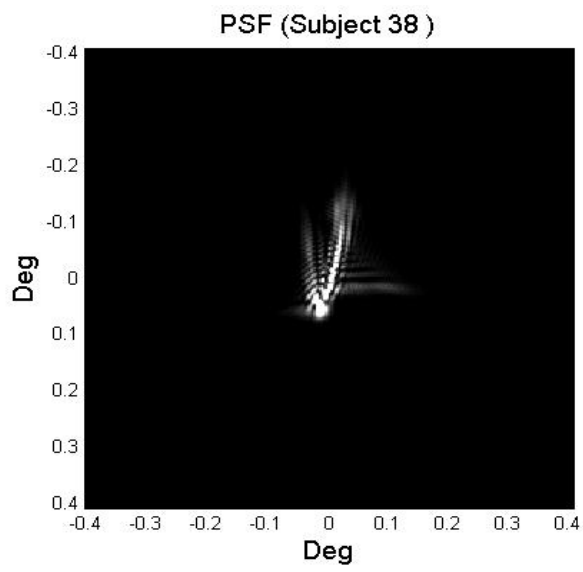
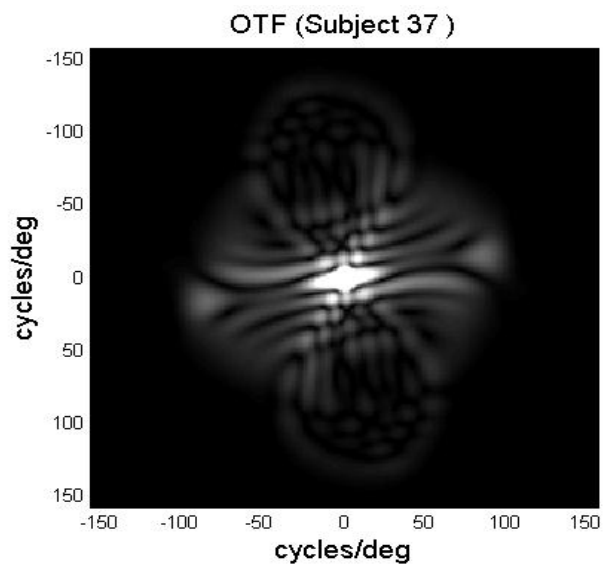
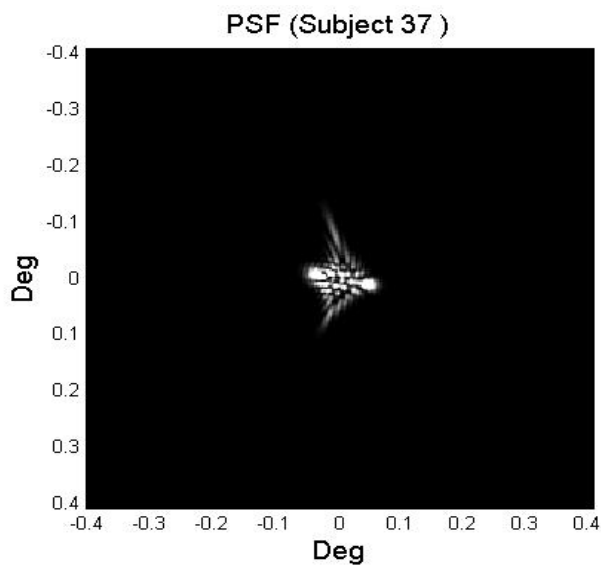
Appendix B

PSF and OTF Images

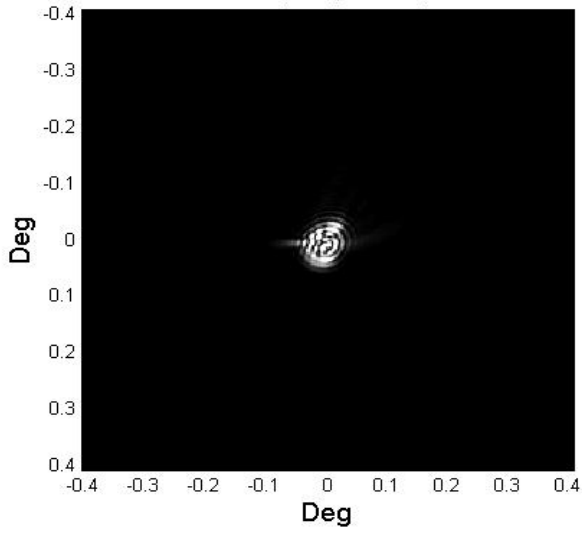




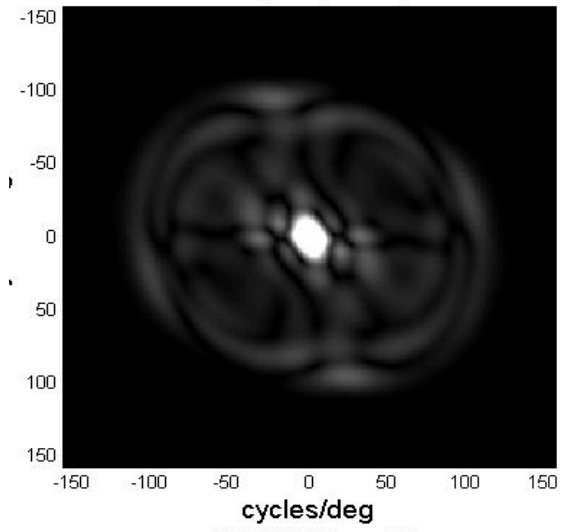




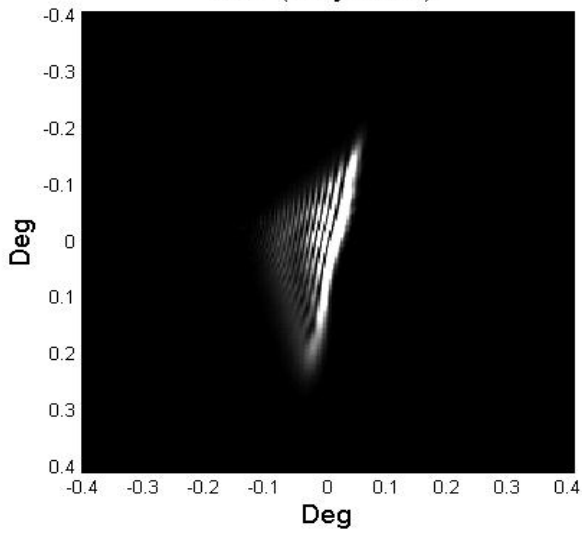
PSF (Subject 47)



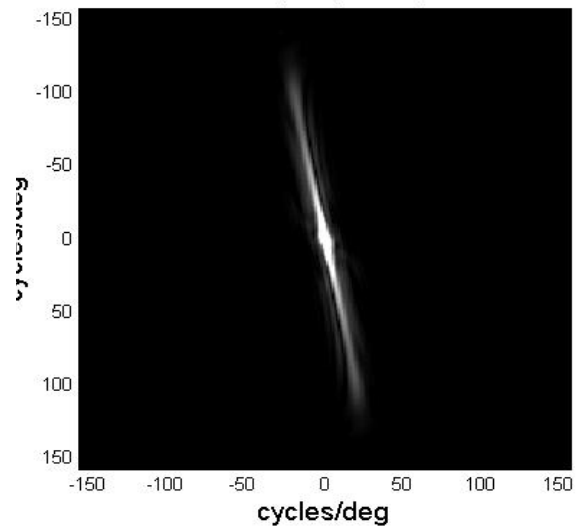
OTF (Subject 47)



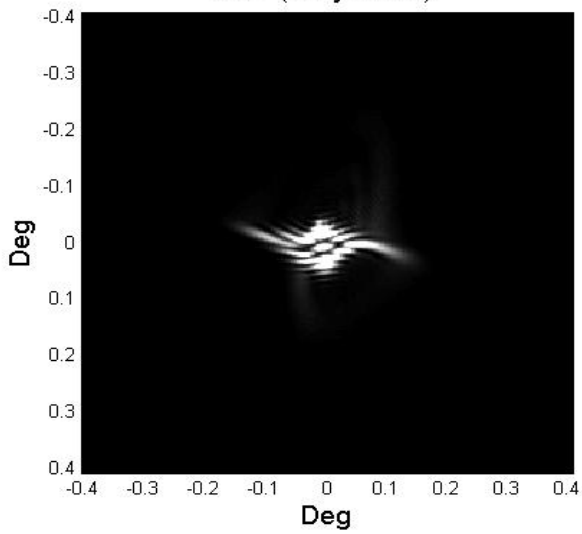
PSF (Subject 49)



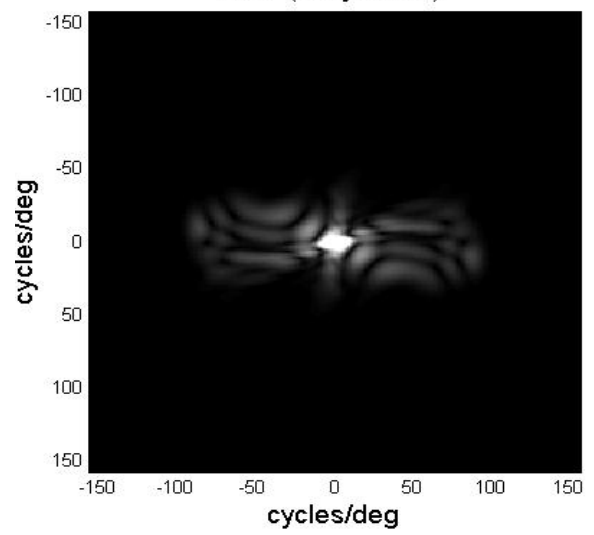
OTF (Subject 49)

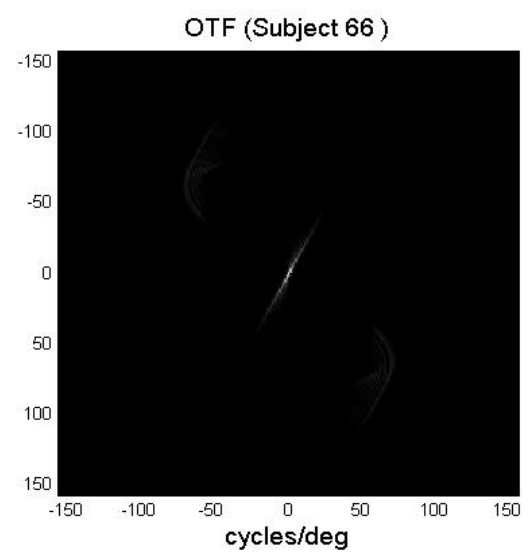
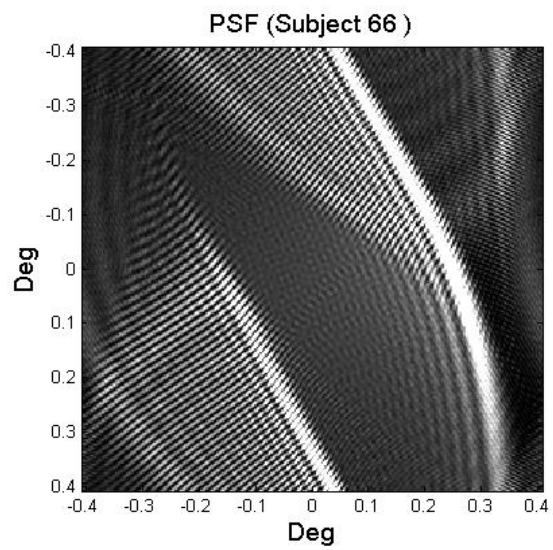
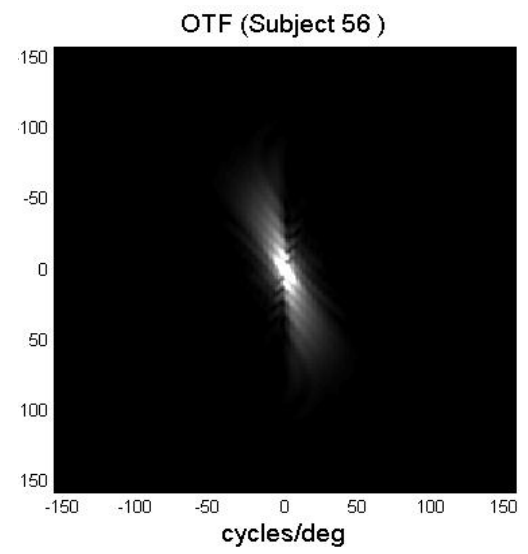
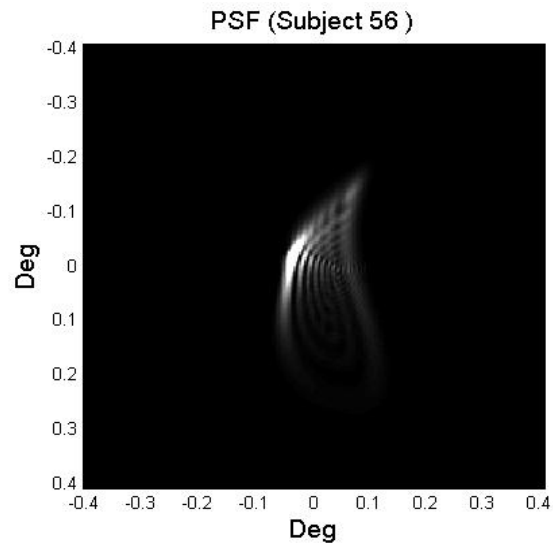
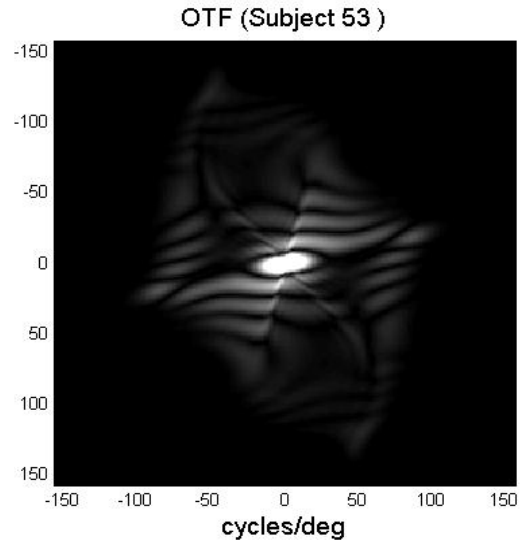
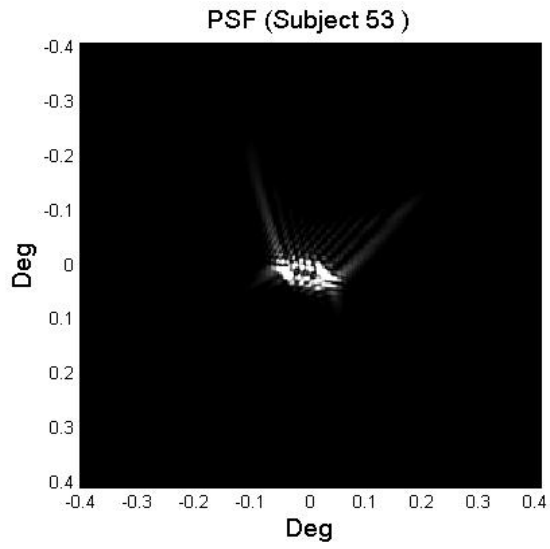


PSF (Subject 50)

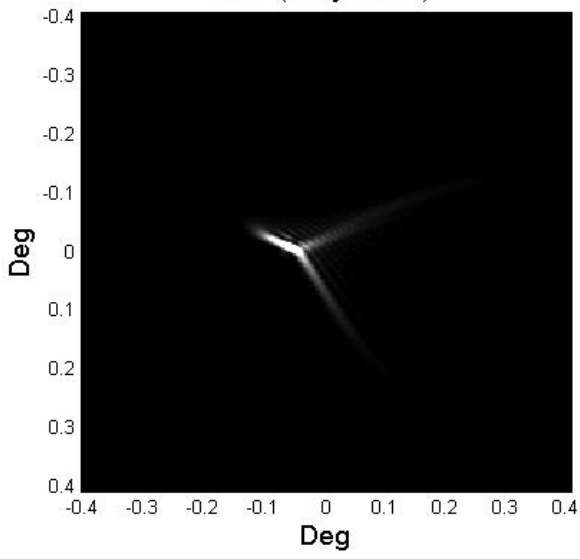


OTF (Subject 50)

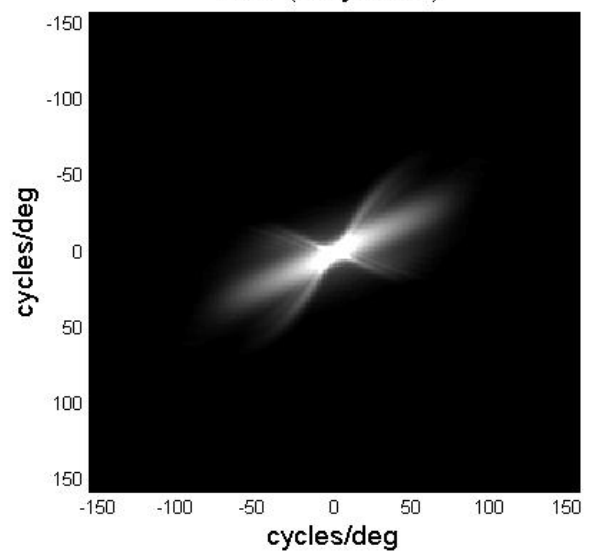




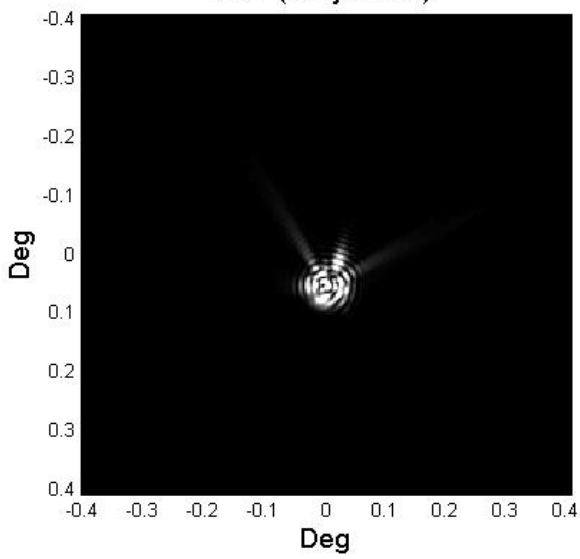
PSF (Subject 87)



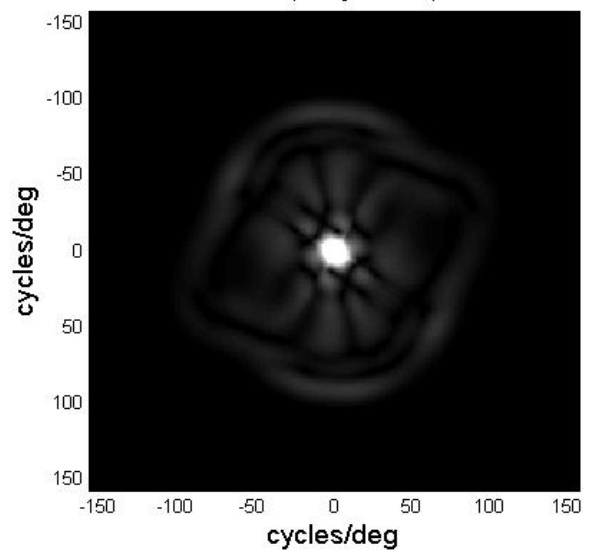
OTF (Subject 87)



PSF (Subject 88)



OTF (Subject 88)



Appendix C

Calculated data to plot psychometric function

Subj # 3; VA=0							
Noise =		20	40	60	80	100	120
Letter sizes	LogMAR	Probability of Correct Response					
5	-0.4	0.2	0.2	0.3	0.2	0.2	0.2
7	-0.3	0.4	0.4	0.4	0.5	0.4	0.4
9	-0.2	0.1	0.1	0.1	0.1	0.1	0.1
11	-0.1	0.7	0.7	0.7	0.7	0.7	0.7
13	0	0.8	0.8	0.9	0.8	0.8	0.8
15	0.1	0.7	0.7	0.7	0.7	0.7	0.7
17	0.2	0.8	0.8	0.8	0.8	0.8	0.8
19	0.3	0.8	0.8	0.8	0.8	0.8	0.8
21	0.4	0.9	0.9	0.9	0.9	0.9	0.9
23	0.5	0.9	0.9	0.9	0.9	0.9	0.9
Thresholds=0.5		-0.13	-0.13	-0.14	-0.15	-0.14	-0.14
0.6	Calculated VA :	-0.07	-0.07	-0.06	-0.07	-0.07	-0.07
0.66		-0.02	-0.02	0.00	-0.02	-0.02	-0.02
RMS Error							
Experimental VA		0.10	0.10	0.10	0.14	0.13	0.13
=	6/6	0.05	0.05	0.04	0.08	0.08	0.08
	0	0.01	0.01	0.00	0.05	0.05	0.05

Subj # 4; VA=0							
Noise =		20	40	60	80	100	120
Letter sizes	LogMAR	Probability of Correct Response					
5	-0.4	0.3	0.3	0.3	0.2	0.3	0.4
7	-0.3	0.2	0.2	0.2	0.2	0.2	0.2
9	-0.2	0.3	0.2	0.2	0.3	0.2	0.3
11	-0.1	0.8	0.8	0.8	0.8	0.8	0.7
13	0	0.7	0.7	0.7	0.7	0.7	0.7
15	0.1	0.7	0.7	0.7	0.7	0.7	0.7
17	0.2	0.9	0.9	0.8	0.9	0.9	1
19	0.3	0.9	0.9	0.9	1	1	1
21	0.4	1	1	1	1	1	1
23	0.5	0.9	0.9	0.9	0.9	0.9	0.8
Thresholds=0.5		-0.16	-0.14	-0.14	-0.15	-0.14	-0.16
0.6	Calculated	-0.09	-0.07	-0.06	-0.09	-0.07	-0.09
0.66	VA :	-0.05	-0.03	-0.02	-0.06	-0.03	-0.04
RMS Error							
Experimental VA		0.11	0.10	0.10	0.11	0.10	0.11
=	6/6	0.06	0.05	0.04	0.07	0.05	0.06
	0	0.03	0.02	0.01	0.04	0.02	0.03

Subj #12; VA=0							
Noise =		20	40	60	80	100	120
Letter sizes	LogMAR	Probability of Correct Response					
5	-0.4	0.2	0.2	0.2	0.3	0.2	0.3
7	-0.3	0.3	0.2	0.3	0.2	0.4	0.2
9	-0.2	0.1	0.1	0.1	0.1	0.1	0.1
11	-0.1	0.8	0.7	0.8	0.7	0.5	0.5
13	0	0.8	0.7	0.7	0.7	0.7	0.7
15	0.1	0.8	0.8	0.8	0.7	0.8	0.8
17	0.2	0.7	0.7	0.7	0.7	0.7	0.7
19	0.3	0.7	0.7	0.7	0.8	0.7	0.7
21	0.4	0.9	0.9	0.8	0.8	0.9	0.8
23	0.5	0.8	0.8	0.9	0.9	0.8	0.8
Thresholds=0.5	Calculated VA	-0.15	-0.14	-0.13	-0.11	-0.09	-0.08
0.6		-0.11	-0.12	-0.07	-0.03	-0.01	-0.01
0.66		-0.07	-0.11	-0.04	0.02	0.05	0.04
		RMS Error					
Experimental VA	6/6 = 0	0.11	0.10	0.10	0.07	0.07	0.06
		0.08	0.09	0.06	0.02	0.01	0.01
		0.05	0.08	0.03	0.02	0.04	0.03

Subj#13; VA=0							
Noise =		20	40	60	80	100	120
Letter sizes	LogMAR	Probability of Correct Response					
5	-0.4	0.2	0.2	0.2	0.2	0.1	0.2
7	-0.3	0.4	0.4	0.4	0.5	0.4	0.4
9	-0.2	0.1	0.1	0.1	0.2	0.1	0.1
11	-0.1	0.6	0.6	0.6	0.7	0.6	0.6
13	0	0.9	1	0.8	0.9	0.9	1
15	0.1	0.7	0.7	0.7	0.7	0.7	0.7
17	0.2	0.9	0.9	0.9	0.8	0.9	0.9
19	0.3	0.9	0.9	0.9	0.9	0.9	1
21	0.4	0.9	1	0.9	1	0.9	0.9
23	0.5	1	0.9	1	1	1	1
Thresholds=0.5	Calculated VA	-0.13	-0.15	-0.12	-0.18	-0.13	-0.15
0.6		-0.07	-0.09	-0.05	-0.10	-0.08	-0.09
0.66		-0.03	-0.06	-0.01	-0.05	-0.04	-0.06
		RMS Error					
Experimental VA	6-/6- 0.00	0.09	0.10	0.08	0.12	0.09	0.10
		0.05	0.07	0.04	0.07	0.05	0.06
		0.02	0.04	0.00	0.03	0.03	0.04

Subj#14; VA=0							
Noise =		20	40	60	80	100	120
Letter sizes	LogMAR	Probability of Correct Response					
5	-0.4	0.1	0.1	0.1	0.1	0.1	0.1
7	-0.3	0.4	0.4	0.3	0.4	0.4	0.4
9	-0.2	0.1	0.1	0.1	0.1	0.2	0.1
11	-0.1	0.6	0.6	0.6	0.6	0.5	0.5
13	0	0.6	0.8	0.7	0.8	0.7	0.7
15	0.1	0.7	0.7	0.7	0.7	0.7	0.6
17	0.2	0.8	0.8	0.8	0.8	0.9	0.8
19	0.3	0.9	1	1	1	1	1
21	0.4	1	1	1	0.9	0.9	1
23	0.5	0.9	0.9	0.9	0.8	0.8	0.9
Thresholds=0.5		-0.08	-0.11	-0.09	-0.12	-0.11	-0.07
0.60	Calculated VA	0.00	-0.05	-0.03	-0.06	-0.04	0.01
0.66		0.04	-0.01	0.01	-0.02	0.00	0.05
		RMS Error					
Experimental VA	6/6	0.05	0.08	0.06	0.08	0.07	0.05
	0	0.00	0.04	0.02	0.04	0.03	0.00
		0.03	0.01	0.01	0.01	0.00	0.04

Subj #15; VA=0							
Noise =		20	40	60	80	100	120
Letter sizes	LogMAR	Probability of Correct Response					
5	-0.4	0.2	0.2	0.2	0.2	0.2	0.2
7	-0.3	0.3	0.3	0.3	0.3	0.3	0.3
9	-0.2	0.1	0.1	0.1	0.1	0.1	0.1
11	-0.1	0.4	0.3	0.2	0.3	0.2	0.3
13	0	0.7	0.7	0.6	0.6	0.6	0.7
15	0.1	0.8	0.7	0.7	0.7	0.7	0.7
17	0.2	0.6	0.6	0.6	0.6	0.6	0.6
19	0.3	0.6	0.6	0.6	0.6	0.6	0.6
21	0.4	0.7	0.7	0.6	0.7	0.7	0.6
23	0.5	0.8	0.8	0.8	0.8	0.8	0.8
Thresholds=0.5		-0.04	-0.02	-0.03	0.01	0.15	-0.02
0.6	Calculated VA	0.03	0.09	0.02	0.13	0.03	0.10
0.66	=	0.12	0.19	0.28	0.23	0.24	0.23
		RMS Error					
Experimental VA =	6/6	0.03	0.01	0.02	0.01	0.11	0.01
	0	0.02	0.07	0.01	0.09	0.02	0.07
		0.08	0.14	0.20	0.16	0.17	0.16

Subj #19; VA=0							
Noise =		20	40	60	80	100	120
Letter sizes	LogMAR	Probability of Correct Response					
5	-0.4	0.2	0.2	0.1	0.2	0.1	0.2
7	-0.3	0.5	0.6	0.6	0.6	0.5	0.5
9	-0.2	0.2	0.2	0.2	0.2	0.2	0.2
11	-0.1	0.8	0.8	0.8	0.8	0.8	0.7
13	0	0.9	0.9	0.9	0.9	0.9	0.8
15	0.1	1	1	1	1	1	1
17	0.2	0.9	0.9	0.9	0.9	0.9	0.9
19	0.3	0.9	0.8	0.8	0.9	0.8	0.8
21	0.4	1	1	1	1	1	0.9
23	0.5	1	1	1	1	1	1
Thresholds = 0.5	Calculated VA=	-0.2	-0.22	-0.21	-0.22	-0.19	-0.19
0.6		-0.153	-0.16	-0.16	-0.17	-0.15	-0.127
0.66		-0.12	-0.129	-0.129	-0.129	-0.12	-0.09
		RMS Error					
Experimental VA =	6/6 0	0.14	0.16	0.15	0.16	0.13	0.13
		0.11	0.11	0.11	0.12	0.11	0.09
		0.08	0.09	0.09	0.09	0.08	0.06

Subj #28; VA=0							
Noise =		20	40	60	80	100	120
Letter sizes	LogMAR	Probability of Correct Response					
5	-0.4	0.1	0.1	0.1	0.1	0.1	0.1
7	-0.3	0.3	0.3	0.2	0.3	0.3	0.2
9	-0.2	0.1	0.1	0.1	0.1	0.1	0.1
11	-0.1	0.5	0.5	0.5	0.5	0.4	0.5
13	0	0.7	0.7	0.7	0.7	0.7	0.7
15	0.1	0.7	0.7	0.7	0.6	0.7	0.6
17	0.2	0.9	0.7	0.9	0.8	0.8	0.7
19	0.3	0.8	0.8	0.8	0.8	0.8	0.8
21	0.4	1	0.9	0.9	1	0.9	0.8
23	0.5	0.9	0.8	0.8	0.7	0.9	0.9
Thresholds=0.5	Calculated VA	-0.08	-0.07	-0.08	-0.07	-0.06	-0.05
0.6		-0.02	-0.007	-0.033	0	0.008	0.01
0.66		0.022	0.04	0.001	0.05	0.05	0.062
		RMS Error					
Experimental VA =	6/6 0	0.06	0.05	0.06	0.05	0.04	0.04
		0.01	0.00	0.02	0.00	0.01	0.01
		0.02	0.03	0.00	0.04	0.04	0.04

Subj #30; VA=0.176							
Noise =		20	40	60	80	100	120
Letter sizes	LogMAR	Probability of Correct Response					
5	-0.4	0.2	0.2	0.2	0.2	0.2	0.2
7	-0.3	0.6	0.5	0.5	0.3	0.3	0.2
9	-0.2	0.4	0.3	0.2	0.2	0.4	0.3
11	-0.1	0.9	0.9	0.7	0.8	0.7	0.8
13	0	0.7	0.7	0.7	0.7	0.7	0.7
15	0.1	1	1	1	1	1	1
17	0.2	0.9	0.9	0.9	0.9	1	0.9
19	0.3	1	1	1	1	1	0.9
21	0.4	0.9	0.9	0.9	0.9	0.9	0.9
23	0.5	0.9	0.9	0.9	0.9	0.9	0.9
Thresholds=0.5	Calculated VA	-0.26	-0.22	-0.18	-0.16	-0.18	-0.17
0.6		-0.20	-0.17	-0.12	-0.12	0.13	0.13
0.66		0.163	-0.13	-0.08	-0.09	-0.13	-0.01
		RMS Error					
Experimental VA =	6 / 9 0.176	0.31	0.28	0.25	0.24	0.25	0.24
		0.27	0.24	0.21	0.21	0.03	0.03
		0.01	0.22	0.18	0.19	0.22	0.13

Subj # 37; VA=0.176							
Noise =		20	40	60	80	100	120
Letter sizes	LogMAR	Probability of Correct Response					
5	-0.4	0.2	0.2	0.2	0.2	0.2	0.2
7	-0.3	0.8	0.8	0.7	0.7	0.7	0.6
9	-0.2	0.1	0.1	0.1	0.1	0.1	0.1
11	-0.1	0.8	0.8	0.7	0.7	0.8	0.7
13	0	0.8	0.9	0.9	0.8	0.9	0.8
15	0.1	0.7	0.7	0.7	0.7	0.7	0.7
17	0.2	0.9	0.9	0.9	0.9	0.9	0.9
19	0.3	0.9	0.9	0.9	0.9	0.9	0.9
21	0.4	0.9	0.9	0.9	0.9	0.9	0.9
23	0.5	1	1	1	0.9	0.9	0.9
Thresholds=0.5	Calculated VA	-0.28	-0.3	-0.24	-0.2	-0.22	-0.17
0.6		-0.09	-0.11	-0.06	-0.1	-0.14	-0.09
0.66		0.011	-0.008	0.031	-0.044	-0.093	-0.038
		RMS Error					
Experimental VA =	6/9 0.176	0.32	0.34	0.29	0.27	0.28	0.24
		0.19	0.20	0.17	0.20	0.22	0.19
		0.12	0.13	0.10	0.16	0.19	0.15

Subj # 38; VA=0.176								
Noise =		20	40	60	80	100	120	
Letter sizes	LogMAR	Probability of Correct Response						
5	-0.4	0.2	0.2	0.2	0.2	0.2	0.2	
7	-0.3	0.4	0.3	0.3	0.4	0.3	0.3	
9	-0.2	0.1	0.1	0.1	0.1	0.1	0.2	
11	-0.1	0.7	0.5	0.6	0.5	0.4	0.4	
13	0	0.8	0.7	0.7	0.8	0.6	0.6	
15	0.1	0.7	0.7	0.7	0.7	0.7	0.7	
17	0.2	0.8	0.8	0.8	0.8	0.8	0.7	
19	0.3	0.7	0.7	0.7	0.7	0.7	0.6	
21	0.4	0.9	0.9	0.8	0.9	0.8	0.8	
23	0.5	0.9	0.8	0.9	0.9	0.8	0.9	
Thresholds=0.5	Calculated VA	-0.14	-0.08	-0.10	-0.10	-0.04	-0.02	
0.60		-0.07	0.00	-0.02	-0.02	0.04	0.08	
0.66		-0.17	0.05	-0.03	0.04	0.10	0.16	
		RMS Error						
Experimental VA =		6/9	0.10	0.06	0.07	0.07	0.03	0.02
		0.176	0.05	0.00	0.02	0.01	0.03	0.06
			0.12	0.04	0.02	0.02	0.07	0.11

Subj # 46; VA=0.176								
Noise =		20	40	60	80	100	120	
Letter sizes	LogMAR	Probability of Correct Response						
5	-0.4	0.1	0.1	0.1	0.1	0.1	0.1	
7	-0.3	0.5	0.4	0.4	0.4	0.4	0.4	
9	-0.2	0.2	0.2	0.2	0.2	0.1	0.3	
11	-0.1	0.8	0.8	0.8	0.8	0.8	0.8	
13	0	0.9	0.9	0.9	0.9	1	0.9	
15	0.1	0.9	0.9	0.9	0.9	0.8	0.9	
17	0.2	0.9	0.9	0.9	0.9	0.9	0.9	
19	0.3	0.9	0.9	0.9	0.9	0.9	0.9	
21	0.4	1	0.9	0.9	0.9	0.9	0.9	
23	0.5	0.9	0.9	0.9	0.9	0.9	0.9	
Thresholds=0.5	Calculated VA	-0.194	-0.18	-0.18	-0.18	-0.161	-0.197	
0.6		-0.146	-0.14	-0.14	-0.14	-0.129	-0.155	
0.66		-0.115	-0.112	-0.112	-0.112	-0.108	-0.127	
		RMS Error						
Experimental VA		6/9	0.26	0.25	0.25	0.25	0.24	0.26
=		0.176	0.23	0.22	0.22	0.22	0.22	0.23
			0.21	0.20	0.20	0.20	0.20	0.21

Subj # 47; VA=0							
Noise =		20	40	60	80	100	120
Letter sizes	LogMAR	Probability of Correct Response					
5	-0.4	0.2	0.2	0.2	0.2	0.2	0.2
7	-0.3	0.2	0.2	0.2	0.2	0.2	0.2
9	-0.2	0.1	0.1	0.1	0.1	0.1	0.1
11	-0.1	0.3	0.2	0.3	0.3	0.3	0.3
13	0	0.7	0.6	0.7	0.7	0.6	0.7
15	0.1	0.7	0.7	0.7	0.7	0.7	0.7
17	0.2	0.7	0.7	0.7	0.7	0.7	0.7
19	0.3	0.7	0.7	0.7	0.7	0.7	0.7
21	0.4	1	1	1	0.9	1	1
23	0.5	0.8	0.8	0.8	0.8	0.7	0.7
Thresholds=0.5	Calculated VA	-0.03	0.007	-0.03	-0.03	-0.01	-0.04
0.6		0.04	0.08	0.04	0.03	0.06	0.03
0.66		0.09	0.122	0.09	0.08	0.11	0.08
		RMS Error					
Experimental VA	6/6 = 0	0.02	0.01	0.02	0.02	0.01	0.03
		0.03	0.05	0.03	0.02	0.04	0.02
		0.06	0.09	0.06	0.06	0.08	0.05

Subj # 49; VA=0							
Noise =		20	40	60	80	100	120
Letter sizes	LogMAR	Probability of Correct Response					
5	-0.4	0.1	0.1	0.1	0.1	0.1	0.1
7	-0.3	0.3	0.3	0.3	0.3	0.3	0.3
9	-0.2	0.2	0.2	0.2	0.2	0.2	0.1
11	-0.1	0.2	0.2	0.2	0.2	0.3	0.2
13	0	0.5	0.5	0.5	0.5	0.5	0.5
15	0.1	0.5	0.4	0.4	0.5	0.4	0.4
17	0.2	0.6	0.5	0.5	0.5	0.6	0.5
19	0.3	0.7	0.7	0.7	0.6	0.6	0.6
21	0.4	0.9	0.8	0.8	0.7	0.6	0.7
23	0.5	0.7	0.7	0.7	0.6	0.7	0.6
Thresholds=0.5	Calculated VA	0.146	0.189	0.189	0.228	0.126	0.252
0.6		0.26	0.302	0.302	0.362	0.229	0.374
0.66		0.32	0.361	0.361	0.432	0.45	0.438
		RMS Error					
Experimental VA	6/6 = 0	0.10	0.13	0.13	0.16	0.09	0.18
		0.18	0.21	0.21	0.26	0.16	0.26
		0.23	0.26	0.26	0.31	0.32	0.31

Subj#50; VA=0							
Noise =		20	40	60	80	100	120
Letter sizes	LogMAR	Probability of Correct Response					
5	-0.4	0.1	0.1	0.1	0.1	0.1	0.1
7	-0.3	0.5	0.5	0.4	0.4	0.4	0.4
9	-0.2	0.3	0.1	0.2	0.3	0.1	0.1
11	-0.1	0.7	0.7	0.7	0.6	0.6	0.6
13	0	0.7	0.7	0.7	0.7	0.8	0.7
15	0.1	0.8	0.8	0.8	0.7	0.8	0.8
17	0.2	0.9	0.9	0.9	0.8	0.8	0.8
19	0.3	0.8	0.8	0.8	0.8	0.8	0.8
21	0.4	0.9	1	0.9	0.9	1	0.9
23	0.5	0.9	0.9	0.9	0.9	0.9	0.9
Threshold=0.5 0.6 0.66	Calculated VA =	-0.18	-0.14	-0.15	-0.13	-0.12	-0.11
		-0.11	-0.07	-0.09	-0.06	-0.07	-0.05
		0.06	-0.03	-0.05	-0.002	-0.027	-0.003
		RMS Error					
Experimental VA =	6/6 0	0.13	0.10	0.10	0.09	0.09	0.08
		0.08	0.05	0.06	0.04	0.05	0.03
		0.05	0.02	0.03	0.00	0.02	0.00

Subj#53; VA=0							
Noise =		20	40	60	80	100	120
Letter sizes	LogMAR	Probability of Correct Response					
5	-0.4	0.2	0.2	0.2	0.2	0.2	0.2
7	-0.3	0.3	0.3	0.3	0.3	0.2	0.3
9	-0.2	0.2	0.2	0.2	0.2	0.2	0.2
11	-0.1	0.7	0.7	0.7	0.6	0.6	0.6
13	0	0.8	0.7	0.8	0.8	0.8	0.7
15	0.1	0.7	0.7	0.8	0.7	0.8	0.7
17	0.2	0.8	0.8	0.8	0.8	0.8	0.8
19	0.3	0.7	0.7	0.7	0.7	0.7	0.7
21	0.4	0.9	0.9	0.9	0.9	0.9	0.9
23	0.5	1	1	1	1	1	1
Thresholds=0.5 0.6 0.66	Calculated VA =	-0.14	-0.12	-0.15	-0.07	-0.12	-0.1
		-0.08	-0.04	-0.1	0.07	-0.07	-0.01
		-0.03	0.012	0.05	0.15	-0.03	0.04
		RMS Error					
Experimental VA =	6/6 0	0.10	0.08	0.11	0.05	0.08	0.07
		0.05	0.03	0.07	0.05	0.05	0.01
		0.02	0.01	0.04	0.10	0.03	0.03

Subj#56; VA=0.176							
Noise =		20	40	60	80	100	120
Letter sizes	LogMAR	Probability of Correct Response					
5	-0.4	0.1	0.1	0.1	0.1	0.1	0.1
7	-0.3	0.4	0.3	0.4	0.3	0.4	0.4
9	-0.2	0.4	0.3	0.2	0.3	0.2	0.1
11	-0.1	0.6	0.6	0.6	0.6	0.6	0.6
13	0	0.6	0.7	0.7	0.6	0.6	0.6
15	0.1	0.7	0.7	0.6	0.6	0.6	0.7
17	0.2	0.7	0.7	0.7	0.7	0.7	0.7
19	0.3	0.8	0.8	0.8	0.8	0.8	0.8
21	0.4	0.9	0.9	0.9	0.9	0.9	0.9
23	0.5	0.8	0.8	0.8	0.8	0.8	0.8
Thresholds=0.5	Calculated VA	-0.14	-0.13	-0.101	-0.09	-0.08	-0.08
0.6		-0.04	-0.06	-0.013	-0.005	-0.02	-0.005
0.66		0.022	-0.002	0.05	0.07	0.09	0.06
		RMS Error					
Experimental VA =	6/9 0.176	0.22	0.22	0.20	0.19	0.18	0.18
		0.15	0.17	0.13	0.13	0.14	0.13
		0.11	0.13	0.09	0.07	0.06	0.08

Subj#66; VA= 0.3							
Noise =		20	40	60	80	100	120
Letter sizes	LogMAR	Probability of Correct Response					
5	-0.4	0.1	0.1	0.1	0.1	0.1	0.1
7	-0.3	0.2	0.2	0.2	0.2	0.2	0.2
9	-0.2	0.2	0.2	0.2	0.2	0.2	0.2
11	-0.1	0.1	0.1	0.1	0.2	0.2	0.2
13	0	0.1	0.1	0.1	0.1	0.1	0.1
15	0.1	0.4	0.5	0.5	0.3	0.3	0.3
17	0.2	0.2	0.2	0.1	0.1	0.1	0.1
19	0.3	0.4	0.5	0.3	0.2	0.1	0.1
21	0.4	0.4	0.4	0.4	0.4	0.3	0.3
23	0.5	0.7	0.7	0.5	0.5	0.1	0.1
Thresholds=0.5	Calculated VA	0.4	0.4	0.52	0.5	0.46	0.46
0.6		0.47	0.47	0.56	0.5	0.49	0.49
0.66		0.5	0.52	0.61	0.57	0.49	0.49
		RMS Error					
Experimental VA =	6/12 0.3	0.09	0.06	0.16	0.14	0.11	0.11
		0.12	0.12	0.19	0.11	0.13	0.13
		0.14	0.15	0.22	0.19	0.14	0.14

Subj#87; VA=0.176							
Noise =		20	40	60	80	100	120
Letter sizes	LogMAR	Probability of Correct Response					
5	-0.4	0.1	0.1	0.2	0.1	0.1	0.2
7	-0.3	0.5	0.5	0.5	0.5	0.4	0.5
9	-0.2	0.3	0.2	0.3	0.3	0.2	0.2
11	-0.1	0.6	0.6	0.5	0.5	0.5	0.5
13	0	0.8	0.7	0.7	0.8	0.7	0.8
15	0.1	0.8	0.8	0.8	0.8	0.8	0.8
17	0.2	1	1	1	1	1	1
19	0.3	0.9	0.9	0.9	0.9	0.9	0.9
21	0.4	0.9	0.9	0.9	0.9	0.9	0.9
23	0.5	1	1	1	1	1	1
Thresholds=0.5	Calculated VA	-0.17	-0.14	-0.15	-0.15	-0.11	-0.15
0.6		-0.11	-0.07	-0.07	-0.09	-0.05	-0.08
0.66		-0.07	-0.03	-0.02	-0.045	-0.012	-0.031
		RMS Error					
Experimental VA =	6/9 0.176	0.24	0.22	0.23	0.23	0.20	0.23
		0.20	0.17	0.17	0.19	0.16	0.18
		0.17	0.15	0.14	0.16	0.13	0.15

Subj#88; VA=0.3							
Noise =		20	40	60	80	100	120
Letter sizes	LogMAR	Probability of Correct Response					
5	-0.4	0.2	0.2	0.2	0.2	0.2	0.2
7	-0.3	0.4	0.3	0.4	0.3	0.4	0.3
9	-0.2	0.1	0.1	0.1	0.1	0.1	0.1
11	-0.1	0.4	0.4	0.3	0.3	0.3	0.1
13	0	0.6	0.6	0.6	0.6	0.6	0.6
15	0.1	0.7	0.7	0.7	0.7	0.7	0.6
17	0.2	0.6	0.6	0.6	0.7	0.6	0.6
19	0.3	0.7	0.7	0.7	0.6	0.6	0.6
21	0.4	0.8	0.8	0.8	0.7	0.7	0.8
23	0.5	0.7	0.8	0.7	0.7	0.7	0.7
Thresholds=0.5	Calculated VA	-0.03	-0.02	-0.005	-0.01	0.007	0.16
0.6		0.09	0.09	0.12	0.1	0.15	0.28
0.66		0.189	0.164	0.21	0.21	0.3	0.35
		RMS Error					
Experimental VA =	6/12 0.3	0.23	0.23	0.22	0.22	0.21	0.10
		0.15	0.15	0.13	0.14	0.11	0.01
		0.08	0.10	0.06	0.06	0.00	0.04

References

- [1] Kitzman DJ., Operant assessment of visual acuity in the profoundly retarded. M.Sc Thesis Drake University, 1985.
- [2] Smirnov A.P., "An analytical method for the calculation of the aberrations of optical systems", *Optics and Spectroscopy*, vol.102, no.1, pp.132-137, (Jan. 2007).
- [3] Howland HC, Howland B. "A subjective method for the measurement of monochromatic aberrations of the eye." *J Opt Soc Am.*; 67(11):1508-1518 (Nov 1977).
- [4] Porter J, Guirao A, Cox IG, Williams DR. "Monochromatic aberrations of the human eye in a large population." *J Opt Soc Am A Opt Image Sci Vis.*; 18(8):1793-1803 ;(Aug 2001).
- [5] Ning Ling, Xuejun Rao, Cheng Wang, Xiang Yu, Yiyun Hu, "Hartmann-shack wavefront sensor for the human eye aberration." *Proc. SPIE*, Vol. 6018, 60180; (2005).
- [6] Walsh G, Charman WN, Howland HC. "Objective technique for the determination of monochromatic aberrations of the human eye." *J Opt Soc Am A.*; 1(9):987-992; (Sep 1984).
- [7] Watson, A. B., Albert J. Ahumada Jr. "Predicting visual acuity from wavefront aberrations." *Journal of Vision*; 8(4):17, 1–19 (2008).
- [8] Applegate, R. A., Marsack, J. D., Ramos, R., & Sarver, E. J. "Interaction between aberrations to improve or reduce visual performance". *Journal of Cataract and Refractive Surgery*, 29, 1487–1495(2003).
- [9] Albert Alm, Paul Kaufman "Adler's Physiology of eye"; Section 9 Visual Perception; Tenth Edition, Mosby, St. Louis.
- [10] Raasch TW, Bailey IL, Bullimore MA. "Repeatability of visual acuity measurement." *Optom VisSci.* 75(5):342-348; (May 1998).
- [11] Hazel CA, Elliott DB. "The dependency of logMAR visual acuity measurements on chart design and scoring rule." *Optom Vis Sci.*; 79(12):788-792 (Dec 2002).
- [12] Born, M., Wolf, E. "Principles of Optics", sixth ed. Pergamon, New York (1980).
- [13] Welford W. T., "Aberrations of optical systems, Human eye. Bristol ;Boston : A. Hilger, c1986.
- [14] Thibos LN, Applegate RA, Schwinger ling JT, Webb R. "Standards for reporting the optical aberrations of eyes". *J Refract Surge*; 18:S652–S661 (2002).
- [15] Thibos LN, Xin Hong, Arthur Bradley, and Xu Cheng "Statistical Variation of Aberration Structure and Image Quality in a Normal Population of Healthy Eyes" *Journal of the Optical Society of America*, 13 (July 2000)
- [16] Luis Alberto Carvalho, "Accuracy of Zernike Polynomials in Characterizing Optical Aberrations and the Corneal Surface of the Eye" *IOVS*. 46:1915-1926;(2005).
- [17] Walsh, G. and Charman, W. "Measurement of the axial wavefront aberration of the human eye". *Ophthal Physiol Opt*, 5, 23-31(1985).

- [18] Applegate RA, Sarver EJ, Khemsara V. "Are all aberrations equal?" J Refract Surge; 18:S556–S562; (2002).
- [19] Nam, Jayoung; Rubinstein, Jacob "Weighted Zernike expansion with applications to the optical aberration of the human eye". J. OSA. A, Optics, vol. 22, no. 9, pp. 1709-16, (September 2005).
- [20] J.S. McLellana, P.M. Prietob, S. Marcosc and S.A. Burnsa "Effects of interactions among wave aberrations on optical image quality." Vis Res, Vol 46, Issue 18, Pages 3009-3016 (September 2006).
- [21] Ye, N., Zhang, X.X., Thibos, L.N. and Bradley, A. (1993) "A new single-surface model eye that accurately predicts chromatic and spherical aberrations of the human eye." Investigative Ophthalmology & visual science; vol.34, no.4, pp.774-774, (1993).
- [22] Smith, W. Modern optical engineering. McGraw-Hill, New York (2000).
- [23] DA Atchison, G Smith, "Optics of the Human Eye", Oxford; Boston: Butterworth-Heinemann, (2000).
- [24] Roorda, A., & Williams, D. R. "The arrangement of the three cone classes in the living human eye." Nature, 397, 520–522 ;(1999).
- [25] Tan Donald T. H., Fong Allan; "Efficacy of neural vision therapy to enhance contrast sensitivity function and visual acuity in low myopia". Journal of Cataract and Refractive Surgery Vol. 34, Issue 4, Pages 570-577 ;(April 2008).
- [26] Yamane N, Miyata K, Samejima T, et al. "Ocular higher-order aberrations and contrast sensitivity after conventional laser in situ keratomileusis". Invest Ophthalmology Vis Sci 2004; 45:3986–3989.
- [27] Thomas T.Norton, Vasudevan Lakshminarayanan, Corliss D, Bailey, J., Butterworth's, Boston, and Carl J. Bassi. Psychophysical Foundations of Visual Perception, ed; Chapter 6:"Spatial Vision"., 2002
- [28] Van Meeteren, A. "Calculations on the optical modulation transfer function of the human eye for white light." Optica Acta, 21, 395-5412(1974).
- [29] Jennings, J. A. M. & Charman, W. N. "An analytical approximation for the modulation transfer functions of the eye." British Journal of Physiological Optics; 29, 64-72(1974).
- [30] Rubinstein, R. Y.; Kroese, D. P. Simulation and the Monte Carlo Method (2nd Ed.). New York: John Wiley & Sons. ISBN; 9780470177938 ;(2007).
- [31] Watson, A. B., & Fitzhugh, A. E. "Modeling character legibility". Society for Information Display Digest of Technical Papers, 20, 360–363(1989).
- [32] Thibos, L. N., Hong, X., Bradley, A., & Applegate, R. A. "Accuracy and precision of objective refraction from wavefront aberrations." Journal of Vision, 4(4):9, 329–351; (2004).
- [33] Jonathan Grainger, Arnaud Reya and Stéphane Dufau "Letter perception: from pixels to pandemonium" Trends in Cognitive Sciences. Volume 12, Issue 10, Pages 381-387;(2008)
- [34] Watson, A. B., & Pelli, D. G. "A Bayesian adaptive psychometric method". Perception & Psychophysics, 33, 113–120. (1983).
- [35] Guirao, A., & Williams, D. R. "A method to predict refractive errors from wave aberration data." Optometry and Vision Science, 80, 36–42 ;(2003).

- [36] Cheng, X., Bradley, A., & Thibos, L. N. "Predicting subjective judgment of best focus with objective image quality metrics." *Journal of Vision*, 4(4):7, 310–321(2004).
- [37] Cheng X, Bradley A, Hong X, Thibos LN. "Relationship between refractive error and monochromatic aberrations of the eye". *Optom Vis Sci*. 80(1):43-49 Jan (2003).
- [38] Marsack, J. D., Thibos, L. N., & Applegate, R. A. "Metrics of optical quality derived from wave aberrations predict visual performance". *Journal of Vision*, 4(4):8, 322–328 ;(2004).
- [39] Nestares, O., Navarro, R., & Antona, B. "Bayesian model of Snellen visual acuity." *Journal of the Optical Society of America A, Optics, Image Science, and Vision*, 20, 1371–1381; (2003).
- [40] Watson, A. B., & Solomon, J. A. "Psychophysics: Mathematica notebooks for psychophysical experiments".*Spatial Vision*, 10, 447–466; (1997).
- [41] Fred M. Dickey and Louis A. Romero; "Normalized correlation for pattern recognition". *Optics Letters*, Vol. 16, Issue 15, pp. 1186-1188 ;(1991).
- [42] Watson, A. B., Albert J. Ahumada Jr., "A standard model for foveal detection of spatial contrast" *Journal of Vision* (2005) 5, 717–740(2005).
- [43] IJspeert, J. K., van den Berg, T. J., & Spekreijse, H., "An improved mathematical description of the foveal visual point spread function with parameters for age, pupil size and pigmentation" *Vision Research*,33, 15–20 (1993).
- [44] "Psychometric function" http://en.wikipedia.org/wiki/Psychometric_function.
- [45] Szwed, M; Cohen, L; Qiao, E ; Dehaene, S "The role of invariant line junctions in object and visual word recognition". *VISION RESEARCH* 49 (7): 718-725 (APR 2009).
- [46] Bach M, Kommerell G. "Determining visual acuity using European normal values: scientific principles and possibilities for automatic measurement". *Klin Monatsbl Augenheilkd*; 212(4):190-5; (Apr1998).
- [47] Jing-hui Li, Yin-xia Han, "Phenomenon of stochastic resonance caused by multiplicative asymmetric dichotomous noise". *Physical Review E; (Statistical, Nonlinear, Soft Matter physics)*,vol.74,no.5,pp.51115-5119;(Nov. 2006)
- [48] Artal, Pablo; Chen, Li; Fernández, Enrique J.; Singer, Ben; Manzanera, Silvestre1; Williams, David R. "Neural compensation for the eye's optical aberrations". *Journal of Vision*. Special Issue: Optics in Vision. Vol 4(4), pp. 281-28 ;(2004).
- [49] Watson, A. B., & Pelli, D. G. QUEST: A Bayesian adaptive psychometric method. *Perception & Psychophysics*, 33, 113–120 (1983).
- [50] Jiang, Jia-Fu; Tan, Rong; Yang, Ding-Qiang "Image Mosaic Based on Contour Feature and Wavelet Transform" *Image and Vision Computing*, vol. 27, no. 4, pp. 469-479, (2009)
- [51] Duda, R. O., & Hart, P. E. "Pattern classification and scene analysis". New York: John Wiley (1973).
- [52] Francisco Castejón-Mochón, José; López-Gil, Norberto; Benito, Antonio1; Artal, Pablo; "Ocular wave-front aberration statistics in a normal young population". *Vision Research*, vol. 42, no. 13, pp. 1611-1617, (June, 2002).
- [53] Smorvik, Dag; Bosnes, Ole "Assessment of visual acuity in preschool children" *Scandinavian Journal of Psychology*. Vol 17(2), pp. 122-124;(1997).

[54] Fern, K. D. & Manny, R. E. "Visual acuity of the preschool child: a review". American Journal of Optometry and Physiological Optics, 63, 319-345; (1986).

[55] Leonid L. Kontsevich, Chien-Chung Chen, Christopher W. Tyler "Separating the effects of response nonlinearity and internal noise psychophysically" Vision Research 42 (2002) 1771–1784

[56] Pelli, Denis G; Majaj, Najib J; Raizman, Noah; Christian, Christopher J; Kim, Edward; Palomares, Melanie C. "Grouping in object recognition: the role of a Gestalt law in letter identification." Cognitive Neuropsychology ;vol:26 iss:1 pg:36 -49;(2009).

[57] Ton, Y; Wysenbeek, YS; Spierer, A "Refractive error in premature infants" Journal of AAPOS [1091-8531];Vol:8iss:6pg:534-538;(2007).

[58] Russell J. Adams, Mary L. Courage "Using a single test to measure human contrast sensitivity from early childhood to maturity" Vision Research 42; P.1205–1210; (2002).

[59] Shute RH, Leat SJ, Westall CA. Assessing Children's Vision, Oxford; Boston: Butterworth-Heinemann (1999).